Landslide susceptibility assessment of the City of Karlovac using the bivariate statistical analysis

Marko Sinčić[1]; Sanja Bernat Gazibara[2]; Martin Krkač[3]; Snježana Mihalić Arbanas[4]

[1] University of Zagreb, Faculty of Mining, Geology and Petroleum Engineering, Pierottijeva 6, 10000 Zagreb, Croatia, ORCID 0000-0003-4252-3523

[2] University of Zagreb, Faculty of Mining, Geology and Petroleum Engineering, Pierottijeva 6, 10000 Zagreb, Croatia, ORCID 0000-0002-5530-4381

[3] University of Zagreb, Faculty of Mining, Geology and Petroleum Engineering, Pierottijeva 6, 10000 Zagreb, Croatia, ORCID 0000-0002-0232-3394

[4] University of Zagreb, Faculty of Mining, Geology and Petroleum Engineering, Pierottijeva 6, 10000 Zagreb, Croatia, ORCID 0000-0003-4036-3722

Abstract

A preliminary landslide susceptibility analysis on a regional scale of 1:100 000 using bivariate statistics was conducted for the City of Karlovac. The City administration compiled landslide inventory used in the analysis based on recorded landslides from 2014 to 2019 that caused significant damage to buildings or infrastructures. Analyses included 17 geofactors relevant to landslide occurrence and classified them into four groups: geomorphological (elevation, slope gradient, slope orientation, terrain curvature, terrain roughness), geological (lithology-rock type, proximity to geological contacts, proximity to faults), hydrological (proximity to drainage network, proximity to springs, proximity to temporary, permanent and to all streams, topographic wetness) and anthropogenic (proximity to traffic infrastructure, land cover using two classifications). Five scenarios were defined using a different combination of geofactors weighted by the Weights-of-Evidence (WoE) method, resulting in five different landslide susceptibility maps. The best landslide susceptibility map was selected upon the results of a ROC curve analysis, which was used to obtain success and prediction rates of each scenario. The novelty in the presented research is that a limited amount of thematic data and an incomplete landslide inventory map allows for the production of a preliminary landslide susceptibility map for usage in spatial planning. Also, this study provides a discussion regarding the used method, geofactors, defined scenarios and reliability of the results. The final preliminary landslide susceptibility map was derived using ten geofactors, which satisfied the pairwise CI test, and it is classified in four zones: low landslide susceptibility (57.05% of the area), medium landslide susceptibility (20.63% of the area), high landslide susceptibility (13.28% of the area), and very high landslide susceptibility (9.03% of the area), and has a success rate of 94% and a prediction rate of 93% making it a highly accurate source of preliminary information for the study area.

1. Introduction

Landslide susceptibility is defined as the spatial, time independent probability of landslides occurring in an area depending on the local terrain conditions (**Guzzetti et al., 1999**; **Guzzetti, 2005**). Landslide susceptibility can be obtained using different analytical approaches, i.e. heuristic, statistical and deterministic (**Soeters and Van Westen, 1996**). Statistical landslide hazard assessment has become very popular, especially with the use of Geographic Information Systems (GIS) and the possibility of applying data integration techniques that have been developed in other disciplines (**Van Westen et al., 2005**). Landslide susceptibility maps are based on the assumption that landslides are likely to occur under the same conditions as those under which they occurred in

the recent past. Due to that reason, the preparation of landslide susceptibility maps requires a landslide inventory map used in combination with a series of environmental factors. All susceptibility maps depict a relative indication of the spatial probability of landslides in the form of zones. A landslide susceptibility map ranks the relative slope stability of an area into categories that range from stable to unstable. The identification and map portrayal of areas highly susceptible to damaging landslides are the first and necessary steps towards loss reduction (**Mihalić Arbanas and Arbanas, 2015**).

The first extensive papers on the use of spatial information in a digital context for landslide susceptibility mapping date back to the late seventies and early eighties of the last century. Among the pioneers in this field were **Brabb et al. (1972)** in California and **Carrara et al. (1977)** in Italy. All research on landslide susceptibility and hazard mapping uses digital tools for handling

Corresponding author: Marko Sinčić
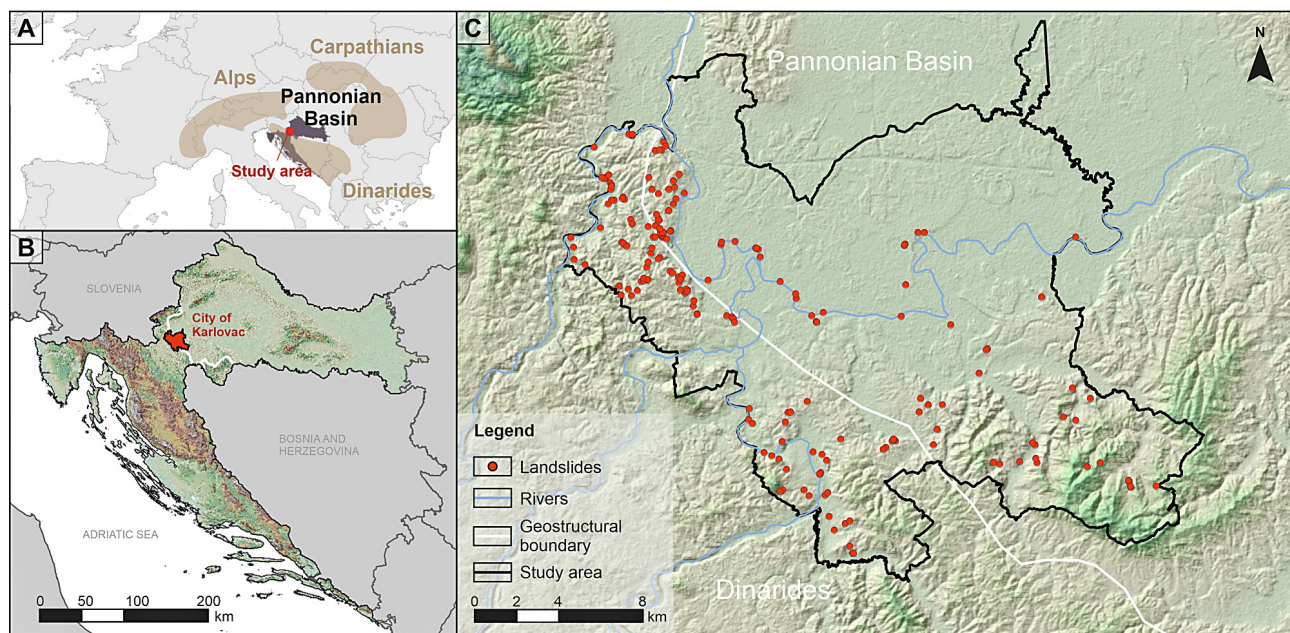*e-mail address: msincic@rgn.hr*

Figure 1: Geographical location of the study area, administrative area of the City of Karlovac in Europe (A) and central Croatia (B). Landslide inventory map of the study area (C).

spatial data, i.e. Geographical Information Systems (GIS). Van Westen's dissertation (**Van Westen, 1993**) is the first comprehensive overview of the application of GIS technology in landslide hazard zonation, followed by the classification of landslide hazard analysis methods. A dissertation by **Guzzetti** (**2006**) provided numerous examples of analysis, assessment and zonation of landslide susceptibility, hazards and risks in Italy, which have been subjects of scientific research. An overview of the spatial data types required for landslide susceptibility assessments and the methods for obtaining these data were published in **Van Westen et al.** (**2008**). The methods and approaches proposed and tested to ascertain landslide susceptibility are shortly presented in **Fell et al. 2008a,b**. Despite numerous attempts and unquestionable progress, the general assumptions and the most popular methods and techniques used to assess landslide susceptibility have not changed significantly in the last few decades (**Guzzetti, 2021**).

Reichenbach et al. (**2018**) critically reviewed the statistically-based landslide susceptibility assessment literature by systematically searching for and then compiling an extensive database of 565 peer-reviewed articles from 1983 to 2016. They have found that the Weight of Evidence (WoE) analysis is among the most common statistical method for landslide susceptibility modelling, together with logistic regression, neural network analysis, data-overlay, index-based and machine learning methods. WoE belongs to bivariate statistical analyses (BSA), one of the simplest statistical analysis methods and it is popular in numerous research fields, enabling environmental scientists to model various natural conditions. BSA techniques can be used as a simple geospatial analysis tool to determine the probabilistic correlation between dependent variables (produced using the inventory map of a landslide incidence) and independent variables (landslide causal factors) by computation of landslide densities and the significance of each factor. In BSA, the importance of each factor is investigated separately (**Porwal et al., 2006; Guzzetti, 2021**).

This paper describes landslide susceptibility modelling by adopting bivariate statistical analysis. The research was performed in the administrative area of the City of Karlovac (total area of 402 km^2), which possesses a database with 196 registered landslides in the form of a landslide inventory map. The study area is characterized by different geological and geomorphological conditions, including lowland and highland areas of the Pannonian Basin and Dinarides (see **Figure 1a,b**). An analyzed landslide inventory map (see **Figure 1c**) contains locations of all landslides registered by the City administration in the period from 2014-2019, and most of them were triggered by rainfall events during Cyclone Tamara (**Mihalić Arbanas et al., 2017**). Landslide and rainfall events are related to extreme weather conditions that are becoming more common in Croatia in recent years (**Bernat Gazibara et al., 2018**), causing material damage in a range of disasters. The application of the Weight of Evidence method, presented in this paper, using a series of landslide causal factors, resulted in the landslide susceptibility map on a small scale of 1:100 000.

The objective of this study is to derive a preliminary landslide susceptibility map on a small scale, using incomplete landslide inventory and limited input data about geofactors, for the application in spatial planning. The main tasks of the research were: (i) optimization of geofactors using a pairwise conditional independence (CI) test; (ii) landslide susceptibility analyses for five
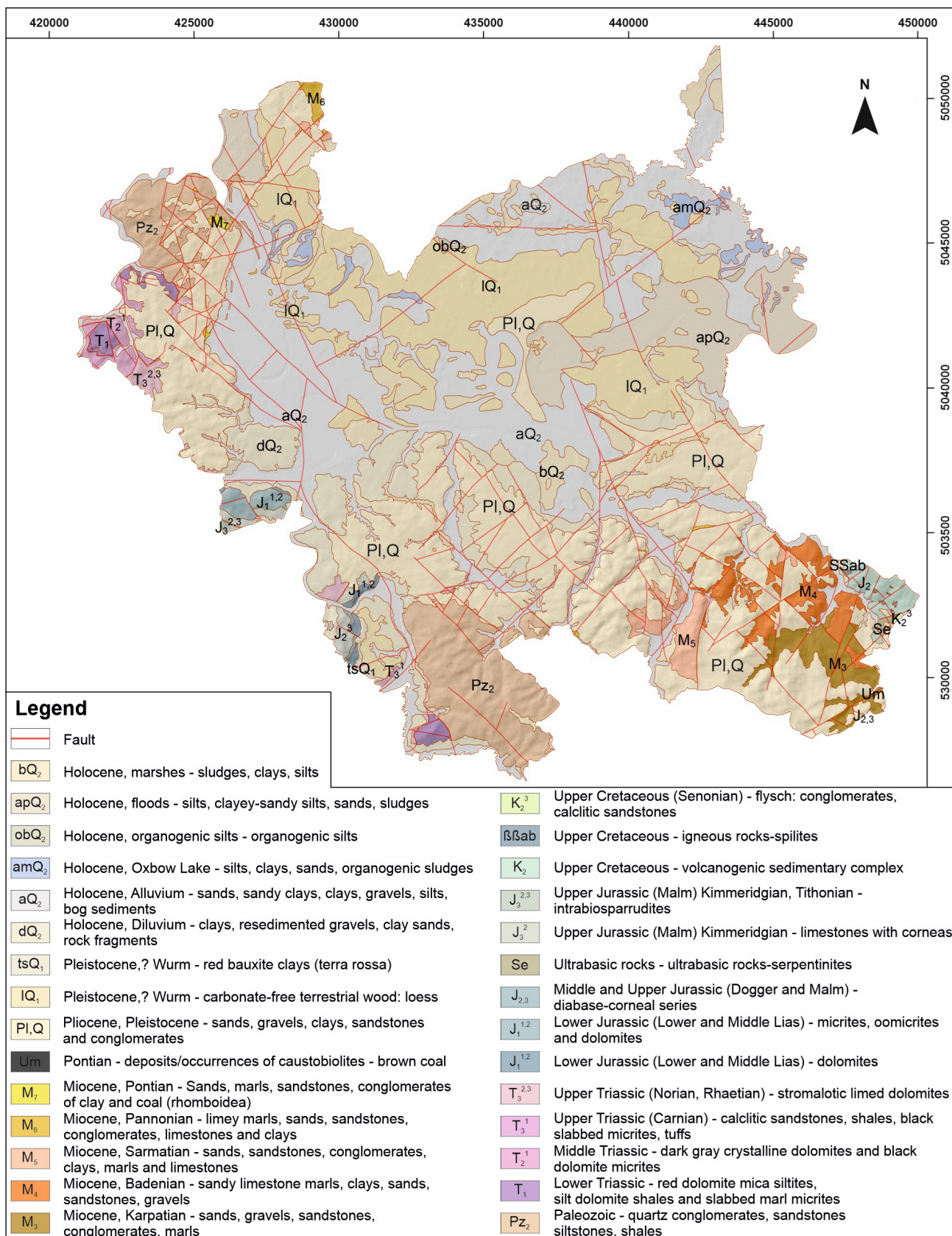
Figure 2: Digitized Basic Geological Map in the scale of 1:100 000 compiled from the Karlovac Sheet (**Benček et al., 1989**) and the Črnomelj Sheet (**Bukovac et al., 1983**)

Legend

Fault	
bQ_2	Holocene, marshes - sludges, clays, silts
apQ_2	Holocene, floods - silts, clayey-sandy silts, sands, sludges
obQ_2	Holocene, organogenic silts - organogenic silts
amQ_2	Holocene, Oxbow Lake - silts, clays, sands, organogenic sludges
aQ_2	Holocene, Alluvium - sands, sandy clays, clays, gravels, silts, bog sediments
dQ_2	Holocene, Diluvium - clays, resedimented gravels, clay sands, rock fragments
tsQ_1	Pleistocene,? Wurm - red bauxite clays (terra rossa)
lQ_1	Pleistocene,? Wurm - carbonate-free terrestrial wood: loess
Pl,Q	Pliocene, Pleistocene - sands, gravels, clays, sandstones and conglomerates
Um	Pontian - deposits/occurrences of caustobiolites - brown coal
M_7	Miocene, Pontian - Sands, marls, sandstones, conglomerates of clay and coal (rhomboidea)
M_6	Miocene, Pannonian - limey marls, sands, sandstones, conglomerates, limestones and clays
M_5	Miocene, Sarmatian - sands, sandstones, conglomerates, clays, marls and limestones
M_4	Miocene, Badenian - sandy limestone marls, clays, sands, sandstones, gravels
M_3	Miocene, Karpatian - sands, gravels, sandstones, conglomerates, marls

K_2^3	Upper Cretaceous (Senonian) - flysch: conglomerates, calclitic sandstones
$ßßab$	Upper Cretaceous - igneous rocks-spilites
K_2	Upper Cretaceous - volcanogenic sedimentary complex
$J_3^{2,3}$	Upper Jurassic (Malm) Kimmeridgian, Tithonian - intrabiosparrudites
J_3^2	Upper Jurassic (Malm) Kimmeridgian - limestones with corneas
Se	Ultrabasic rocks - ultrabasic rocks-serpentinites
$J_{2,3}$	Middle and Upper Jurassic (Dogger and Malm) - diabase-corneal series
$J_1^{1,2}$	Lower Jurassic (Lower and Middle Lias) - micrites, oomicrites and dolomites
$J_1^{1,2}$	Lower Jurassic (Lower and Middle Lias) - dolomites
$T_3^{2,3}$	Upper Triassic (Norian, Rhaetian) - stromalotic limed dolomites
T_3^1	Upper Triassic (Carnian) - calclitic sandstones, shales, black slabbed micrites, tuffs
T_2^1	Middle Triassic - dark gray crystalline dolomites and black dolomite micrites
T_1	Lower Triassic - red dolomite mica siltites, silt dolomite shales and slabbed marl micrites
Pz_2	Paleozoic - quartz conglomerates, sandstones siltstones, shales

scenarios using different combinations of landslide causal factor groups; (iii) verification of all susceptibility maps using AUC rates for defined scenarios. The research was organized to elaborate the assumption that a limited amount of input data can be used for a reliable prediction of "where" landslides are likely to occur.

2. Study area

The study area is defined by the administrative border of the City of Karlovac located in the central part of Croatia, encompassing the area of contact between two geotectonic units of Internal and External Dinarides (**Schmid et al., 2008**; **Tomljenović et al., 2008**) as well as the Pannonian Basin. Geomorphologically, most of the study area belongs to the megageomorphological regions of the Pannonian Basin and, to a lesser extent, to the Dinaridic Mountain System (**Bognar, 2001**). Consequently, the relief generally changes in the northeast-southwest direction from plain (the fluvial floodplain of the Kupa River) through lowland (Crna Mlaka Depression) to hilly type (the hills of Vukomeričke Gorice, Utinjsko-Tušilovički Hills and Vojnić Hills) according to changes of geological settings (**Mihalić Arbanas et al., 2017**). The Karlovac Depression is surrounded by the lowest slopes of Samobor Hills on the northwest, the Vukomeričke Gorice on the northeast and it is separated by the Korana River from Kordun Foothills.

The elevation ranges from 101 to 372 m a.s.l. and the altitude increases to the west, to the southwest and the south, in the direction of relief changes. The prevailing slope angles (70% of the study area) are <5° whereas only 20% of the study area is in a range from 5° to 10° and 9% is in a range from 10° to 20°. The study area comprises 402 km², where the current land cover includes about 20 km² of artificial surfaces, about 200 km² of agricultural areas, and about 180 km² of forests. An area of about 7 km² belongs to water bodies of four large rivers (the Kupa, Korana, Dobra and Mrežnica rivers) and other types of inland waters. The City of Karlovac is the administrative centre of the Karlovac County and its largest urban area with a population of 59,016 residents (**DZS 2011**). The study area is comprised of Quaternary, Neogene and Pre-Neogene sediments and mostly sedimentary rocks.

Figure 2 presents geological characteristics of the City area according to the Basic Geological Map on a scale of 1:100 000, compiled from the Karlovac Sheet (**Benček et al., 1989**) and the Črnomelj Sheet (**Bukovac et al., 1983**). A detailed description of geological units is given in **Madaš et al. (1989)**. Quaternary deposits prevail at the surface of the study area (about 85% of the area). The Holocene sediments are of fluvial origin, composed of sand, sandy clays, clays, gravels, silt and bog sediments. The Pleistocene deposits are loess and heterogeneous mixtures of mostly impermeable clayey soils. The Miocene and Pliocene deposits are present

only at the surface in part of the hilly area (about 4% of the area) in the form of stratified sandstones, conglomerates, marls and limestones, as well as sands, gravels and clays. The Pre-Neogene rocks are composed of Mesozoic deposits of the Triassic, Jurassic and Cretaceous periods (about 4% of the area) and Upper Paleozoic deposits (about 7% of the area). Mesozoic deposits are composed of various types of chemogene, clastic, intrusive, effusive and metamorphic rocks due to complex geotectonic history, including flysh-type rocks. The Upper Paleozoic is composed of quartz conglomerates, sandstones, siltstones and shales.

The City of Karlovac is highly affected by landslide hazards. The climate of the City is continental with a mild maritime influence, with mean annual precipitation (MAP) of 1 100 mm and with precipitation mostly recorded in the period from May to December (**Zaninović et al., 2008**). However, landslides are also controlled by extreme hydrological events, i.e. floods which are caused by regional events, such as Cyclone Tamara from 2014, when the heavy rainfall triggered more than 100 landslides in the Karlovac area during one rainfall event. Due to heterogenic geological and geomorphological conditions, landslide types are of various sizes, from small to medium-large landslides (<10 hectares). The preparatory causal factors of slope instabilities in the study area depend on the geomechanical properties of rocks and soils, geomorphological conditions and processes, including river erosion and different types of man-made processes.

3. Data and methods

This chapter describes input data for landslide susceptibility analyses, including a landslide inventory and spatial data divided into groups of geomorphological, geological, hydrological and anthropogenic geofactors. In this study, bivariate statistics was used to determine landslide susceptibility. The Weight of Evidence method was applied to calculate the weight factors of classes for each factor map and a pairwise test was used to determine factor maps' conditional independence.

3.1. Data

The input data for the landslide susceptibility analysis of the City of Karlovac area includes the landslide inventory and other spatial data used to derive factor maps. Landslide inventory was obtained from the City administration in vector point files indicating the locations of 196 landslides recorded in the period from 2014 to 2019. The landslide inventory was compiled based on information received from citizens or road patrol who informed the City administration responsible for landslide remediation or civil protection. Most reported landslides have damaged infrastructure, mainly roads and private properties. The landslide inventory of the City of Karlovac was split
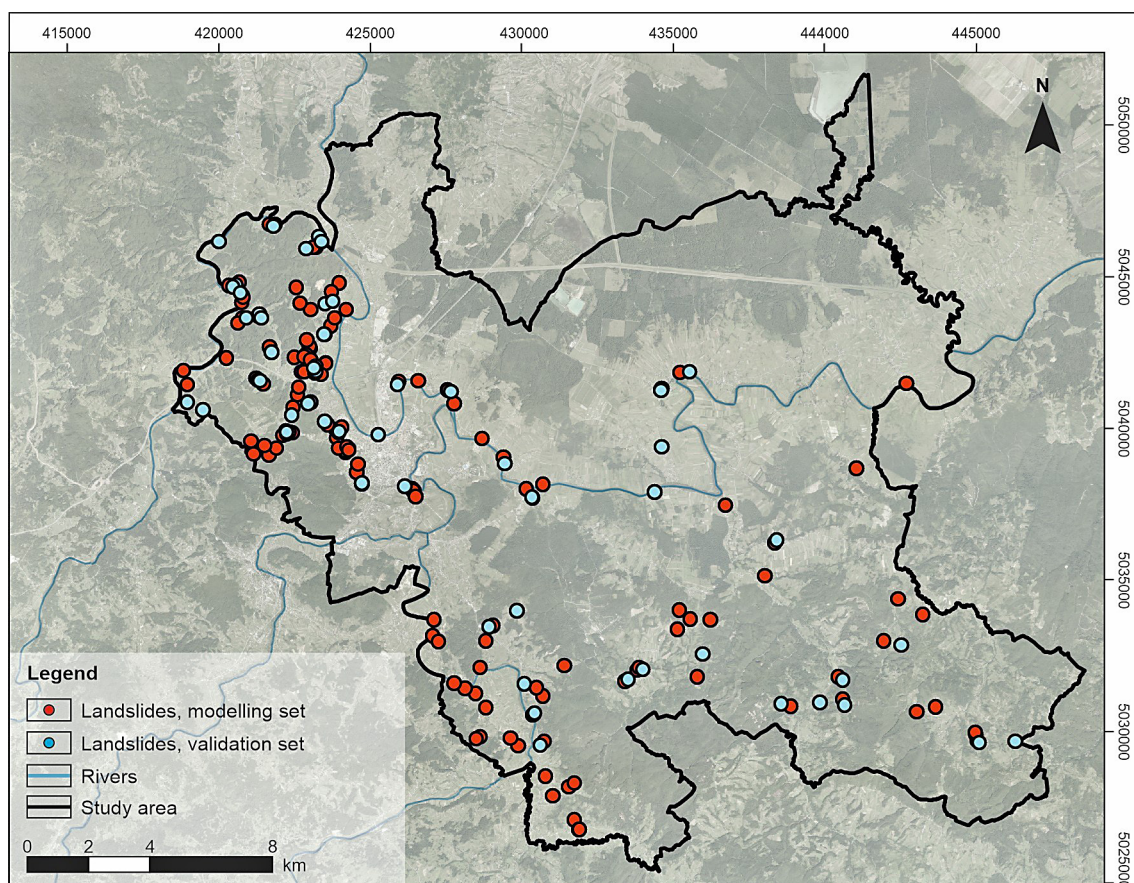
Figure 3: Landslide inventory map (1:250 000) with landslides divided into two sets used for the development of the susceptibility model and its verification

into two data sets by random selection in *ArcGIS 10.8*, a modelling set (140 landslides in the inventory) for modelling landslide susceptibility and a validation set (56 landslides in the inventory) (see **Figure 3**).

The landslide causal factors for the landslide susceptibility modelling in the City were selected expertly and based on data availability. The existing data for this study area includes topography in the form of a Digital Elevation Model (EU-DEM) with a resolution of 25 x 25 m downloaded from Copernicus Land Monitoring Service (**EEA, 2018**), digitalised geologic data from the Basic Geologic Map (**Benček et al., 1989; Bukovac et al., 1983**) in a scale of 1:100 000, digitalised hydrological data (superficial streams and springs) from the topographic map in a scale 1:25 000, land cover data of the CORINE Land Cover dataset (**NRC/LC, 2018**) and traffic infrastructure from Open Street Maps (**OSM, 2019**). Most factor maps are derived by further processing (i.e. geomorphometric, topographic and distance analysis) of the original input data. Only land cover data and geological units are applied as original data in the model. A total of 17 landslide-conditioning factors, such as elevation, slope gradient, slope orientation, terrain curvature, terrain roughness, lithology (rock type), proximity to geological contact and faults, proximity to drainage network, springs, temporary streams, permanent streams and all streams,

topographic wetness, land cover (a), land cover (b) and proximity to traffic infrastructure were used in the study. All analyses were performed in *ArcGIS 10.0* software, where all 17 factor maps were converted to raster format with a spatial resolution of 25 m. The following section describes all derived factor maps.

Elevation is a very frequently used parameter in landslide susceptibility studies because landslides may form in specific relief ranges (**Dai et al., 2001**). The relief map of the study area generated from the EU-DEM is shown in **Figure 4a**. The range of elevations shown on the DEM indicates a difference in altitude of 271 m. A factor map of elevations was created by reclassifying the 25 m resolution DEM.

Slope gradient is often considered to be the most important morphometric parameter used to more effectively analyze and describe relief (**Van Westen et al., 2008**). A slope gradient factor map was created using the *Spatial Analyst* extension (*Slope tool*) in the *ArcGIS 10.0* software, and it represents the spatial distribution of slope angle values in the range from 0 to 90 degrees. The slope values in the study area (see **Figure 4b**) range between 0° and 40°. However, the mean value of the slope is 3.97°, with a standard deviation of 4.04°.

The slope aspect identifies the downslope direction of the maximum rate of change in the elevation value from
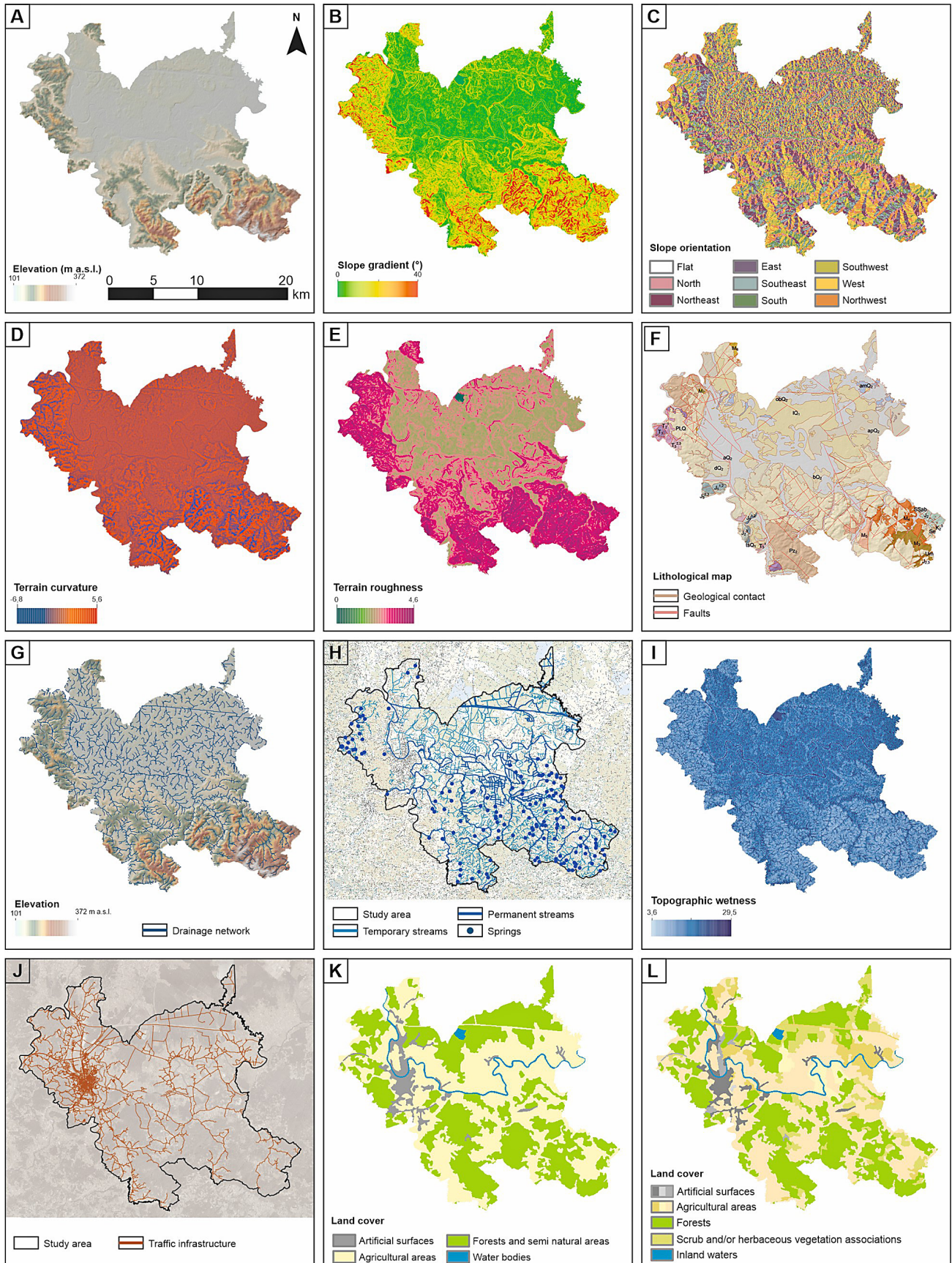
Figure 4: Input data and factor maps used in landslide susceptibility modelling of the City of Karlovac

Table 1: First and second levels of classification of the Corine Land Cover (CLC) (**NRC/LC, 2018**)

The first level of classification	The second level of classification
Artificial surfaces	Urban fabric
	Industrial, commercial and transport units
	Mine, dump and construction sites
	Artificial, non-agricultural vegetated areas
Agricultural areas	Arable land
	Permanent crops
	Pastures
	Heterogeneous agricultural areas
Forest and semi natural areas	Forests
	Scrub and/or herbaceous vegetation associations
	Open spaces with little or no vegetation
Wetlands	Inland wetlands
	Maritime wetlands
Water bodies	Inland waters
	Marine waters

each cell to its neighbours. The resulting aspect dataset with eight main directions, N, NE, E, SE, S, SW, W, NW and flat surfaces (see **Figure 4c**), was created with the *Aspect tool* (*3D Analyst*) in *ArcGIS 10.0* software.

Surface curvature is the curvature of a line formed by intersecting a plane (in some chosen orientation) with the terrain surface. The curvature map was created with the *Curvature tool* (*3D Analyst*) in the *ArcGIS 10.0* software. The curvature shapes define the possible processes on the slopes, whether the flow slows down or accelerates on the slope. The values for the study area vary between -6.84 and 5.64 (see **Figure 4d**). The mean value of the profile curvature data is 2.46, with a standard deviation of 0.96.

A terrain roughness map (see **Figure 4e**) was created using the *Roughness tool* in the *Geomorphometry and Gradient Metrics Toolbox* (**Evans et al., 2014**). Terrain Ruggedness Index (TRI) is defined according to **Riley et al.** (**1999**), and the algorithm calculates the sum change in elevation between a grid cell and its eight neighbour grid cells. Therefore, an increased TRI shows more significant local relief heterogeneity.

Geological data were obtained from the Basic Geological Map on a scale 1:100 000, the Karlovac Sheet (**Benček et al., 1989**) and the Črnomelj Sheet (**Bukovac et al., 1983**). The digitalisation of geological maps and further spatial analysis resulted in three factor maps: lithological map, which shows chronostratigraphic units (see **Figure 4f**); proximity to geological contacts; and proximity to faults. Geological data obtained by digitizing the Basic Geological Map 1:100 000 are shown in **Figure 2.**

A drainage network is a set of all drainage systems in an area, i.e. a set of natural canals through which water constantly flows or temporary, and which are connected into a single stream and represent the smallest independent geomorphological component (**Marković, 1983**). In this paper, the drainage network was derived from a 25 m resolution DEM using several tools in the *Spatial Analyst – Hydrology Toolbox* in *ArcGIS 10.0* and is presented as vector data in the shape of a line, as shown in **Figure 4g**.

The digitalisation of the topographic map with a scale 1:25 000 (TK25) available on the WMS server of the State Geodetic Administration resulted in vector data of superficial streams in the shape of a line and springs in the shape of a point (see **Figure 4h**). Streams were classified as permanent and temporary. Based on the digitalized input data, four factor maps were created: proximity to springs, proximity to (all) streams, proximity to temporary streams and proximity to permanent streams.

Topographic wetness is a steady state wetness index, and it is commonly used to quantify topographic control on hydrological processes. The topographic wetness map was derived from a DEM using the *Compound Topographic Index tool* in *Geomorphometry and Gradient Metrics Toolbox* (**Evans et al., 2014**) in *ArcGIS 10.0* software, and it represents the Compound Topographic Index (CTI) shown in **Figure 4i**. Lower values of CTI indicate lower wetness (hill tops), and higher CTI values indicate higher terrain wetness (plain areas).

The traffic infrastructure network, including roads and railways, is obtained from the Open Street Map website in the form of vector data, as shown in **Figure 4j**. The factor map showing proximity to the traffic infrastructure was created based on the input data.

Information on the land cover was downloaded from the Copernicus Land Monitoring Service (Corine Land Cover) website as accessible raster files ready for use in GIS. Land cover, according to the Corine Land Cover (CLC), is classified into three hierarchically organised levels of detail. The first and second levels of classification were used in this paper, as shown in **Table 1** and **Figure 4k** and **Figure 4l**, respectively. The most detailed third level was not used in the analysis due to the relatively large study area and the small scale of the analysis.

3.2. Methods

Landslide susceptibility is a quantitative or qualitative assessment of the spatial probability of a particular type of landslide to occur in an area. An overview of landslide susceptibility assessment methods is given in many papers, e.g. in **Corominas et al.** (**2013**) and **Reichenbach et al.** (**2018**). Qualitative methods are inventory-based and knowledge-driven methods. Quantitative methods are based on data (data-driven, statistical methods) and on physically-based models. In this paper, a bivariate statistical method referred to as Weights-of-Evidence (**Agterberg et al., 1990; Bonham-Carter et**

al., 1989; Bonham-Carter, 1994) is applied in a GIS environment to derive quantitative spatial information on the predisposition to landslides. Because of the size of the study area (402 km^2) and limited data availability, the WoE method is considered as the appropriate approach. General schematic representation of the processes of map development according to **Van Westen et al. (2002)** is shown in **Figure 5**. Each factor map overlaps with the landslide inventory map for the purpose of obtaining the frequency of landslides in each class of all factors. By comparing the landslide density in the factor classes with the landslide density in the entire study area, the relative influence of the observed landslide factor is determined. After the calculated densities, weighting factors can be determined using different methods (**Coe et al., 2004**). The disadvantage of the bivariate method is that it starts from the assumption that the sliding factors are mutually independent, which is not usually the case in natural environments (**Van Westen et al., 2002**). To mitigate the influence of dependent factors, i.e. violating the conditional independence, a pairwise test is applied to all factor maps and their classes.

The Weight of Evidence method was developed by the Canadian Geological Survey (**Agterberg et al., 1990**; **Bonham-Carter et al., 1989**), and it was used to map mineral resources. **Sabto (1991)** applied the above method to landslide hazard analysis. This method is easy to use in the GIS interface, and **Table 2** shows the variables used to calculate the weighting factors.

Table 2: Defining the variables used in the Weight of Evidence method (modified from **van Westen et al. 2002**)

Landslides	Potential landslide causal factor	
	Present	Absent
Present	Npix$_1$	Npix$_2$
Absent	Npix$_3$	Npix$_4$

The variables shown are four possible combinations obtained after overlapping a landslide map (binary landslide map) with a weight map (binary variable map). After defining the variables, **Equations (1)** and **(2)** are used to calculate the positive and negative weights, respectively. The final weight of evidence value, used for landslide susceptibility analyses, is acquired using **Equation (3)** (**Van Westen et al., 2002**).

$$W_i^+ = \log_e \frac{\dfrac{Npix_1}{Npix_1 + Npix_2}}{\dfrac{Npix_3}{Npix_3 + Npix_4}} \qquad (1)$$

$$W_i^- = \log_e \frac{\dfrac{Npix_2}{Npix_1 + Npix_2}}{\dfrac{Npix_4}{Npix_3 + Npix_4}} \qquad (2)$$

$$W_{map} = W_i^+ - W_i^- + \sum W_i^- \qquad (3)$$

Where:

Npix$_1$ – number of pixels for present landslides and present potential landslide causal factor;

Npix$_2$ – number of pixels for present landslides and absent potential landslide causal factor;

Npix$_3$ – number of pixels for absent landslides and present potential landslide causal factor;

Npix$_4$ – number of pixels for absent landslides and absent potential landslide causal factor;

W$_i^+$ – positive weights (indicating the importance of the presence of the factor);

W$_i^-$ – negative weights (indicating the importance of the absence of the factor);

W$_{map}$ – weight of evidence value (weight factor).

As stated by **Bonham-Carter (1994)**, the pairwise conditional independence (CI) test should be run on all combinations of factor maps used in the analyses using bivariate statistics, i.e. the Weight of Evidence method. The pairwise CI test can reveal the magnitude of violating the assumption of factor maps independence and identify which maps are causing the most dependence. Using **Equations (4)**, **(5)** and **(6)**, the χ_{ab}^2 value is calculated for each pair of the factor maps (*a* and *b*) and later compared to the tabulated values of χ_{ab}^2. The tabulated values depend on the significance level *p* selected expertly and the degree of freedom *d* calculated using **Equation (7)**. Furthermore, for corrections on the factor maps showing dependence, a Yates correction (**Walker and Lev, 1953**) was done according to **Equation (8)**.

$$\chi_{ab}^2 = \sum_{i=1}^{k} \frac{\left(f_{i(o)} - f_{i(e)}\right)^2}{f_{i(e)}} \qquad (4)$$

Where:

a, b – studied factor map a and factor map b, respectively;

k – multiplication of the number of classes in the two studied factor maps

$$\text{i.e.: } k = x \times y \qquad (5)$$

where: x, y – the number of classes in factor map a and factor map b, respectively;

f$_{i(o)}$ – number of observed landslides in the overlap area of two classes of two studied factor maps;

f$_{i(e)}$ – expected number of landslides in the overlap area of two classes of two studied factor maps

$$\text{i.e.: } f_{i(e)} = \frac{\sum_{i=1}^{x} f_{i(o)} \times \sum_{i=1}^{y} f_{i(o)}}{N} \qquad (6)$$

where: N – total amount of observed landslides.

$$d = (x-1) \times (y-1) \qquad (7)$$

$$\chi_{ab}^2 = \sum_{i=1}^{k} \frac{\left(\left|f_{i(o)} - f_{i(e)}\right| - 0.5\right)^2}{f_{i(e)}} \qquad (8)$$

Bivariate statistical analysis

Landslide inventory map

Factor maps

Slope length
Slope convexity
Slope direction
Distance to roads
Distance to streams
Lithology
Slope classes
Geomorphology
Distance to faults
Landuse

Artificial surfaces
Forests
Water

Weight maps

Weight: Slope length
Weight: Slope convexity
Weight: Slope direction
Weight: Distance to roads
Weight: Distance to streams
Weight: Lithology
Weight: Slope classes
Weight: Geomorphology
Weight: Distance to faults
Weights: Landuse

+0,3
-0,4
-2,6

1. Overlay of the first factor map and the landslide inventory map. Calculation of landslide densities for each class and the overall landslide density in the entire map

Slope	Slide	npix.	Density
0-10	No	200	0,01
10-20	No	125	0,05
20-30	Yes	300	1,55
30-40	Yes	150	0,85
40-50	Yes	210	1,20
> 50	Yes	55	0,03

2. Calculate a weight value for each class in the first factor map using:
-information values, or
-weights of evidence, or
-certainty factors
The landslide density in a class is related to the overall landslide density in the map

Slope
Slope
Slope
Proximity to roads
Proximity to streams
Lithology
Slope classes
Geomorphology
Distance to faults
Landuse

Class	Weight
Artificial surfaces	+0,3
Forests	-0,4
Water	-2,4

Weight tables

3. Reclassify the factor map with the weight values stored in the table.
Repeat the procedure 1 to 3 for all factor maps

4. Combine all weight maps into a single map using certain combination rules

Susceptibility range

+6,4

-9,5

100%
50%
0%

-9,5   0   +6,4

low   medium   high

5. Reclassifying the susceptibility range in 3 classes: low, medium and high susceptibility.

6. Overlapping the susceptibility map with the landslide inventory, calculating the landslide density in all three classes of suscepti-bility and adjusting the cut-off values until satisfying results

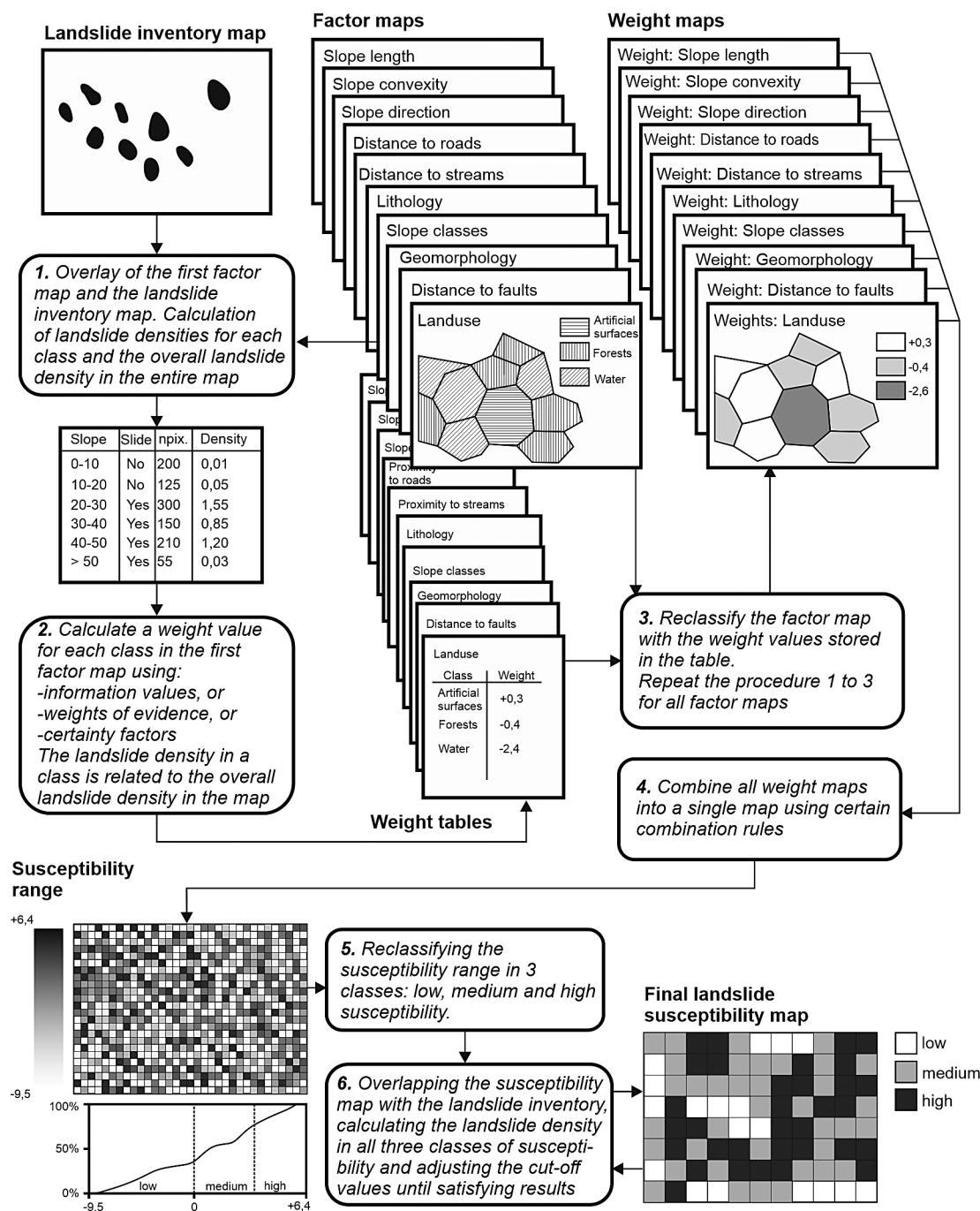**Final landslide susceptibility map**

low
medium
high

Figure 5: Simplified flow chart of the development of landslide susceptibility map using bivariate statistical method (**Van Westen et al., 2002**)

4. Results

The GIS-based landslide susceptibility assessment for the City of Karlovac comprises the following main processing steps: (i) calculation of weights for factor maps using the modelling set of the landslides by applying the Weight of Evidence method; (ii) testing the CI using pairwise test; (iii) calculation of the posterior probability map (i.e. combination of the controlling factors to predict po-tential landslide occurrences); (iv) developing four different scenarios to determine landslide causal factor group importance; (v) modelling validation using the validation set of landslides from the inventory, and (vi) classification of the landslide susceptibility map.

4.1. Weight maps

In this study, 17 factor maps were created for the landslide susceptibility analysis. Derived factor maps

can be divided into four groups of landslide causal factors: (i) geomorphological factors, including an elevation map, a slope gradient map, a slope aspect map, a terrain curvature map, and a terrain roughness map; (ii) geological factors, including a lithology map, proximity to the geological contacts and faults; (iii) hydrological factors, including proximity to the drainage network, springs, temporary streams, permanent streams and all streams and a topographic wetness map; and (iv) anthropogenic factors, including proximity to traffic infrastructure, two land cover maps derived based on the first and second level of hierarchical division. Classes of stretched uncategorical factor maps were defined expertly, and they are listed in the following paragraphs together with the most important relations to landslides.

The elevation map is divided into four classes: 100-150 m a.s.l.; 150-200 m a.s.l.; 200-250 m a.s.l.; and 250-375 m a.s.l. Only four landslides were recorded in the class above 250 m a.s.l., while the class 150-200 m a.s.l. has the greatest impact on the occurrence of landslides.

The slope gradient map is divided into five classes: 0-5°; 5-10°; 10-15°; 15-20°; and 20-40°. The greatest influence on the occurrence of landslides is given by the slope gradient classes 10-15°; and 20-40°, while in the 0-5° class, fewer landslides were observed than expected.

The slope orientation map is divided into nine classes: flat terrain, north (N), northeast (NE), east (E), southeast (SE), south (S), southwest (SW), west (W) and northwest (NW). Landslides were not recorded on flat terrains, while most of them were recorded on slopes oriented to the northeast and south, and it is concluded that these slopes have the greatest impact on the occurrence of landslides.

The terrain curvature map is divided into four classes: concave slopes (-7-0.5); slightly concave slopes (-0.5-0); slightly convex slopes (0-0.5); and convex slopes (0.5-6). According to the results, by far the greatest influence on the occurrence of landslides has the class 0.5-6, the convex slopes.

The terrain roughness map is divided into four classes: smooth terrain (0-1); slightly rough terrain (1-2); rough terrain (2-3); and very rough terrain (3-5). There are only 12 landslides in the class of smooth terrain and very rough terrain (significantly less than the expected number of landslides), while the classes of slightly rough terrain and rough terrain have a significant impact on the occurrence of landslides.

Lithology (rock type) is divided into 29 classes according to the chronostratigraphic units defined on the Basic Geological Map on a scale of 1:100 000 (see **Figure 2**). The class with the most significant influence on the occurrence of landslides are Pliocene and Pleistocene deposits (Pl, Q): sands, gravels, clays, sandstones and conglomerates. A significant number of landslides were recorded in the class of alluvium (aQ_2): sands, sandy clays, clays, gravels, silt, bog sediments.

The proximity to the geological contacts map is divided into five classes: 0 - 50 m; 50 - 100 m; 100 - 200 m; 200 - 400 m; 400 - 800 m; and 800 - 3800 m. In class 0 - 50 m, 49 landslides were recorded, and in class 50 - 100 m, 36 landslides were recorded. Only 4.38 landslides were expected in the mentioned classes, so it is concluded that most landslides occur near the geological contact (from 0 to 100 m). In the class proximity greater than 800 m to the geological contact, 105 landslides were expected, and only 17 were recorded.

The proximity to the fault map is divided into six classes: 0 - 50 m; 50 - 100 m; 100 - 200 m; 200 - 400 m; and 400 - 1600 m. Classes of proximity 0 - 50 m and 50 - 100 m have by far the greatest impact on the occurrence of landslides, 25 and 26 landslides were recorded, respectively, although only 1.84 were expected in each class.

The proximity to the drainage network map is divided into five classes: 0 - 50 m; 50 - 100 m; 100 - 200 m; 200 - 300 m; and 300 - 550 m. The distribution of recorded landslides is significant for analysis in almost all classes of each parameter.

The proximity to springs map is divided into five classes: 0 - 100 m; 100 - 250 m; 250 - 500 m; 500 - 1000 m; and 1000 - 12 000 m. Class 0 - 100 m has a very small area with only one recorded landslide. In the classes 100 - 250 m, 250 - 500 m and 500 - 1000 m, significantly more landslides were recorded than was expected.

The proximity to temporary streams is divided into six classes: 0 - 100 m; 100 - 200 m; 200 - 300 m; 300 - 400 m; 400 - 500 m; and 500 – 2,300 m. Given the difference between the number of mapped and expected landslides, all classes except 500 – 2,300 m indicate the possibility of landslides.

The proximity to permanent streams map is divided into six classes: 0 - 100 m; 100 - 200 m; 200 - 300 m; 300 - 400 m; 400 - 500 m; and 500 - 3,600 m. The greatest impact is given by the class 0 - 100 m because a relatively large number of landslides were recorded near permanent streams.

The proximity to all streams map is divided into six classes: 0 - 100 m; 100 - 200 m; 200 - 300 m; 300 - 400 m; 400 - 500 m; and 500 - 1,800 m. Similar to the proximity to temporary streams map, all classes except the 500 – 1,800 class indicate the possibility of landslides, i.e. have more observed than expected landslides.

The topography wetness map is divided into four classes: dry terrain (3.36 - 6.38); slightly humid terrain (6.38 - 7.09); humid terrain (7.09 - 7.7); and very humid terrain (7.7 - 29.5). The greatest influence on the occurrence of landslides has the class of dry terrain (3.36 - 6.38). However, significantly less than expected has the class of slightly humid terrain (6.38 - 7.09).

The proximity to the traffic infrastructure map is divided into four classes: 0 - 50 m; 50 - 100 m; 100 - 200 m; and 200 - 2,200 m. The class of distance 0 - 50 m from the roads has the largest difference between ex-

Table 3: Calculated weights for landslide causal factors based on the Weight of Evidence method

		Class description	Class area	$Npix_1$	$Npix_2$	$Npix_3$	$Npix_4$	W_i^+	W_i^-	W_{map}
Geomorphological landslide causal factors	Elevation	100-150 m a.s.l.	267.96	66	74	267.96	132.22	-0.35	0.47	-0.66
		150-200 m a.s.l.	79.10	60	80	79.10	321.08	0.77	-0.34	1.28
		200-250 m a.s.l.	33.01	10	130	33.01	367.17	-0.14	0.01	0.01
		250-375 m a.s.l.	20.11	4	136	20.10	380.07	-0.56	0.02	-0.42
		SUM	**400.18**	**140**					**0.17**	
	Slope gradient	0-5°	281.82	64	76	281.82	118.36	-0.43	0.61	-0.74
		5-10°	80.26	45	95	80.26	319.91	0.47	-0.16	0.51
		10-15°	29.13	24	116	29.13	371.05	0.86	-0.11	0.84
		15-20°	7.41	4	136	7.41	392.77	0.43	-0.01	0.32
		20-40°	1.56	3	137	1.56	398.62	1.71	-0.02	1.60
		SUM	**400.18**	**140**					**0.30**	
	Slope orientation	flat terrain	1.16	0	140	1.16	399.53	0.00	0.00	-0.01
		north	51.37	12	128	51.37	349.31	-0.40	0.05	-0.46
		north-east	53.63	29	111	53.63	347.06	0.44	-0.09	0.52
		east	49.27	21	119	49.27	351.42	0.20	-0.03	0.22
		south-east	44.33	16	124	44.33	356.35	0.03	0.00	0.03
		south	44.26	24	116	44.26	356.42	0.44	-0.07	0.50
		south-west	50.35	11	129	50.35	350.33	-0.47	0.05	-0.53
		west	53.46	15	125	53.46	347.23	-0.22	0.03	-0.26
		north-west	52.86	12	128	52.86	347.82	-0.43	0.05	-0.49
		SUM	**400.69**	**140**					**-0.01**	
	Terrain curvature	concave slopes	70.14	28	112	70.14	330.03	0.13	-0.03	0.17
		slightly concave slopes	138.51	30	110	138.51	261.67	-0.48	0.18	-0.66
		slightly convex slopes	127.84	30	110	127.84	272.34	-0.40	0.14	-0.54
		convex slopes	63.68	52	88	63.68	336.49	0.85	-0.29	1.14
		SUM	**400.18**	**140**					**0.01**	
	Terrain roughness	smooth	148.48	4	136	148.48	251.70	-2.56	0.43	-3.13
		slightly rough	165.09	81	59	165.09	235.09	0.34	-0.33	0.67
		rough	77.71	47	93	77.70	322.47	0.55	-0.19	0.74
		very rough	8.91	8	132	8.91	391.27	0.94	-0.04	0.98
		SUM	**400.18**	**140**					**-0.13**	
Geological landslide causal factors	Proximity to the geological contact	0-50m	95.88	49	91	95.88	304.73	0.38	-0.16	0.51
		50-100m	69.96	36	104	69.96	330.65	0.39	-0.11	0.46
		100-200m	90.84	18	122	90.83	309.77	-0.57	0.12	-0.71
		200-400m	89.07	20	120	89.07	311.54	-0.44	0.10	-0.57
		400-1600m	54.86	17	123	54.86	345.75	-0.12	0.02	-0.17
		SUM	**400.61**	**140**					**-0.03**	
	Proximity to faults	0-50m	38.43	25	115	38.43	362.11	0.62	-0.10	0.72
		50-100m	35.24	26	114	35.24	365.30	0.75	-0.11	0.86
		100-200m	60.69	18	122	60.69	339.85	-0.16	0.03	-0.19
		200-400m	85.05	27	113	85.05	315.49	-0.10	0.02	-0.12
		400-800m	87.44	33	107	87.44	313.10	0.08	-0.02	0.10
		800-3800m	93.69	11	129	93.69	306.85	-1.09	0.18	-1.27
		SUM	**400.54**	**140**					**0.00**	

Table 3: Continued

		Class description	Class area	Npix$_1$	Npix$_2$	Npix$_3$	Npix$_4$	W$_i^+$	W$_i^-$	W$_{map}$
Geological landslide causal factors	Lithology (rock type)	bQ$_2$	13.59	1	139	13.59	387.07	-1.56	0.03	-1.65
		apQ$_2$	22.70	1	139	22.70	377.95	-2.07	0.05	-2.19
		obQ$_2$	0.41	0	140	0.41	400.25	0.00	0.00	-0.07
		amQ$_2$	4.06	0	140	4.06	396.59	0.00	0.01	-0.08
		aQ$_2$	110.03	27	113	110.03	290.62	-0.35	0.11	-0.53
		dQ$_2$	26.56	10	130	26.56	374.09	0.07	-0.01	0.01
		tsQ$_1$	0.55	2	138	0.55	400.10	2.34	-0.01	2.29
		lQ$_1$	53.02	5	135	53.02	347.64	-1.31	0.11	-1.48
		Pl. Q	109.26	63	77	109.26	291.40	0.50	-0.28	0.71
		Um	0.01	0	140	0.01	400.65	0.00	0.00	-0.07
		M$_7$	0.42	0	140	0.42	400.23	0.00	0.00	-0.07
		M$_6$	0.69	0	140	0.69	399.97	0.00	0.00	-0.07
		M$_5$	4.25	2	138	4.25	396.40	0.30	0.00	0.23
		M$_4$	6.83	1	139	6.83	393.83	-0.87	0.01	-0.95
		M$_3$	5.76	5	135	5.76	394.89	0.91	-0.02	0.86
		K$_2^3$	0.07	0	140	0.07	400.58	0.00	0.00	-0.07
		ββab	0.11	0	140	0.11	400.54	0.00	0.00	-0.07
		K$_2$	2.95	0	140	2.95	397.71	0.00	0.01	-0.08
		J$_3^{2.3}$	0.23	0	140	0.23	400.42	0.00	0.00	-0.07
		J$_3^2$	1.89	1	139	1.89	398.76	0.41	0.00	0.35
		Se	0.23	0	140	0.23	400.43	0.00	0.00	-0.07
		J$_{2.3}$	0.00	0	140	0.00	400.65	0.00	0.00	-0.07
		J$_1^{1.2}$	2.04	1	139	2.04	398.62	0.34	0.00	0.27
		J$_1^{1.2}$	0.78	3	137	0.78	399.87	2.40	-0.02	2.35
		T$_3^{2.3}$	2.61	4	136	2.61	398.04	1.48	-0.02	1.43
		T$_3^1$	0.07	1	139	0.07	400.59	3.78	-0.01	3.71
		T$_2^1$	2.32	1	139	2.32	398.33	0.21	0.00	0.14
		T$_1$	2.44	1	139	2.44	398.22	0.16	0.00	0.09
		Pz$_2$	26.78	11	129	26.77	373.88	0.16	-0.01	0.11
		SUM	**400.65**	**140**					**-0.07**	

pected and mapped landslides, and it is concluded that the roads contribute to the instability of the slopes. However, it should be considered that most of the landslides were recorded by the municipal warden in charge of road maintenance.

Land cover map A, derived from the first level of hierarchical classification, has four classes: artificial surfaces, agricultural areas; forests and semi-natural areas; and water bodies. In the class of agricultural areas, the expected number of landslides is 68.93, and 106 land-

slides were recorded. From the above, it is concluded that the most significant impact on the occurrence of landslides has the class of agricultural areas.

The land cover map B, derived from the second level of hierarchical classification, is divided into nine classes: urban fabric; industrial, commercial and transport units; artificial, non-agricultural vegetated areas; arable land; pastures; heterogeneous agricultural areas; forests; scrub and/or herbaceous vegetation associations; and inland waters. Almost all mapped landslides are in the

Table 3: Continued

		Class description	Class area	$Npix_1$	$Npix_2$	$Npix_3$	$Npix_4$	W_i^+	W_i^-	W_{map}
Hydrological landslide causal factors	Proximity to the drainage network	0-50m	91.92	26	114	91.92	308.12	-0.21	0.06	-0.27
		50-100m	83.50	22	118	83.50	316.53	-0.28	0.06	-0.35
		100-200m	136.27	39	101	136.27	263.76	-0.20	0.09	-0.30
		200-300m	71.55	47	93	71.55	328.49	0.63	-0.21	0.84
		300-550m	16.80	6	134	16.80	383.24	0.02	0.00	0.02
		SUM	**400.04**	**140**					**0.00**	
	Proximity to springs	0-100m	4.72	1	139	4.72	395.96	-0.50	0.00	-0.43
		100-250m	22.23	18	122	22.23	378.44	0.84	-0.08	0.99
		250-500m	56.91	18	122	56.91	343.76	-0.10	0.02	-0.04
		500-1000m	90.12	34	106	90.12	310.55	0.08	-0.02	0.17
		1000-12000	226.69	69	71	226.69	173.99	-0.14	0.16	-0.22
		SUM	**400.68**	**140**					**0.07**	
	Proximity to temporary streams	0-100m	135.65	23	117	135.65	264.54	-0.72	0.23	-0.95
		100-200m	98.98	27	113	98.98	301.21	-0.25	0.07	-0.31
		200-300m	63.30	19	121	63.30	336.89	-0.15	0.03	-0.17
		300-400m	39.06	19	121	39.06	361.13	0.33	-0.04	0.39
		400-500m	22.74	7	133	22.74	377.45	-0.13	0.01	-0.12
		500-2300m	40.47	45	95	40.47	359.72	1.16	-0.28	1.45
		SUM	**400.19**	**140**					**0.01**	
	Proximity to permanent streams	0-100m	62.75	31	109	62.75	337.60	0.35	-0.08	0.36
		100-200m	49.76	11	129	49.76	350.60	-0.46	0.05	-0.57
		200-300m	42.29	17	123	42.29	358.06	0.14	-0.02	0.09
		300-400m	36.09	7	133	36.09	364.26	-0.59	0.04	-0.69
		400-500m	31.08	3	137	31.08	369.27	-1.29	0.06	-1.41
		500-3600m	178.38	71	69	178.37	221.98	0.13	-0.12	0.19
		SUM	**400.35**	**140**					**-0.06**	
	Proximity to all streams	0-100m	179.41	44	96	179.41	220.37	-0.36	0.22	-0.51
		100-200m	104.41	24	116	104.41	295.36	-0.42	0.11	-0.47
		200-300m	52.43	17	123	52.43	347.34	-0.08	0.01	-0.02
		300-400m	26.29	18	132	26.29	373.48	-0.14	0.01	-0.08
		400-500m	13.09	9	131	13.09	386.69	0.67	-0.03	0.77
		500-1800	13.09	38	102	24.14	375.64	1.50	-0.25	1.82
		SUM	**399.78**	**96**					**0.07**	
	Topographic wetness	dry	83.76	64	76	83.76	316.42	0.78	-0.38	1.05
		slightly humid	135.07	57	83	135.07	265.11	0.19	-0.11	0.19
		humid	115.69	11	129	115.69	284.49	-1.30	0.26	-1.67
		very humid	65.65	8	132	65.65	334.52	-1.05	0.12	-1.28
		SUM	**400.18**	**140**					**-0.11**	

class of heterogeneous agricultural areas, 104 of them, which makes this class the most susceptible to landslides. Landslides were not recorded in the classes industrial, commercial and transport units, artificial, non-agricultural, vegetated areas and arable land.

4.2. Pairwise CI test

Pairwise conditional independence (CI) test between all classes of all causal factors was tested using the pairwise CI test before deriving landslide susceptibility maps.

Table 4 shows χ^2 values calculated for each combination of weight maps using **Equations 4**, **5** and **6**. Tabulated χ^2 values are acquired by calculating the degree of freedom (see **Equation 7**) for the significance level of 1%.

Conditional independence or conditional dependence for each pair of weight maps is determined by comparing the two χ^2 values. Greater calculated χ^2 value than the tabulated shows that the pair has conditional dependence, i.e. the null hypothesis of conditional independence is rejected.

Table 3: Continued

		Class description	Class area	Npix$_1$	Npix$_2$	Npix$_3$	Npix$_4$	W$_i^+$	W$_i^-$	W$_{map}$
Anthropogenic landslide causal factors	Proximity to traffic infrastructure	0-50m	71.94	123	17	71.94	328.27	1.59	-1.91	2.49
		50-100m	53.61	4	136	53.61	346.59	-1.55	0.11	-2.66
		100-200m	80.18	3	137	80.18	320.02	-2.24	0.20	-3.44
		200-2200m	194.47	10	130	194.47	205.73	-1.92	0.59	-3.51
		SUM	**400.20**	**140**					**-1.00**	
	Land cover (A)	Artificial surfaces	19.57	13	127	19.57	381.08	0.64	-0.05	0.35
		Agricultural areas	197.26	106	34	197.26	203.40	0.43	-0.74	0.83
		Forest and semi natural areas	176.51	13	127	176.50	224.15	-1.56	0.48	-2.38
		Water bodies	7.32	8	132	7.32	393.33	1.14	-0.04	0.84
		SUM	**400.66**	**140**					**-0.34**	
	Land cover (B)	urban fabric	14.71	13	127	14.71	385.95	0.93	-0.06	0.57
		industrial. commercial and transport units	4.59	0	140	4.59	396.07	0.00	0.01	-0.43
		artificial. non-agricultural vegetated areas	0.28	0	140	0.28	400.38	0.00	0.00	-0.42
		arable land	11.48	0	140	11.48	389.18	0.00	0.03	-0.45
		pastures	23.95	2	138	23.95	376.71	-1.43	0.05	-1.89
		heterogeneous agricultural areas	161.83	104	36	161.83	238.83	0.61	-0.84	1.03
		forests	146.10	11	129	146.10	254.56	-1.53	0.37	-2.32
		scrub and/or herbaceous vegetation associations	30.40	2	138	30.40	370.25	-1.67	0.06	-2.15
		inland waters	7.32	8	132	7.32	393.33	1.14	-0.04	0.76
		SUM	**400.66**	**140**					**-0.42**	

Firstly, weight maps that contain similar information are reduced to one map. For example, between four maps proximity to drainage network, proximity to temporary streams, proximity to permanent streams and proximity to all streams, only one map is chosen as optimal weight map, proximity to drainage network because it was derived using a DEM thus including both geomorphological and hydrological information. Land cover (A) is rejected as it showed a more conditional dependence with other weight maps compared to the land cover (B). Besides, weight maps that showed significant conditional dependence with the remaining weight maps were excluded. This filtering resulted in removing the elevation, the slope gradient and the terrain curvature weight map, as they showed conditional dependence with several remaining weight maps. Finally, for the remaining conditional dependent weight map pairs, the Yates correction (**Equation 8**) is applied, resulting in less CI violation. The Yates correction is necessary to apply for small expected frequencies (**Bonham-Carter, 1994**), however, in this paper, it was applied for the mitigation of CI limitations, reducing the amount of dependence pairs. **Table 5** shows the final selection of weight maps after the three-step filtering used for landslide susceptibility modelling.

4.3. Landslide susceptibility modelling, verification and zonation

For each class of the selected factor maps listed in **Table 5**, a weight value was defined applying the WoE method resulting in the W_{map} value (see **Table 3**). This study created the landslide susceptibility maps by summing (overlapping) the factor maps according to the assigned weight values based on five scenarios. The first, Scenario 0, is used to create the final landslide susceptibility map as it contains all the weight maps which passed the three-step filtering. The other four scenarios are defined to determine which landslide causal factor group has the most significance to landslide susceptibility modelling. Therefore, in each of the four scenarios (Scenario I-IV) different group of landslide causal factors is used, as shown in **Table 6**.

The success and prediction rate of all scenarios was determined for all five landslide susceptibility maps, and the results are shown in **Table 6**. Furthermore, ROC curves for Scenario 0 used for the final susceptibility map are shown in **Figure 6,** presenting the success and prediction rates. Scenario 0 was selected as the optimal in order to use all eight weight maps which passed the three-step filtering for the final landslide susceptibility map. How-

Table 4: Calculated and tabulated χ² values for all weight map pairs

	Elevation	Slope gradient	Slope orientation	Terrain curvature	Terrain roughness	Lithology (rock type)	Prox. to geol. contact	Prox. to faults	Prox. to drainage network	Proximity to springs	Prox. to temporary streams	Prox. to permanent streams	Prox. to all streams	Topographic wetness	Prox. to traffic infrastructure	Land cover (A)
Slope gradient	**30** / *26*															
Slope orientation	**27** / *43*	**22** / *53*														
Terrain curvature	**52** / *22*	**28** / *26*	**32** / *43*													
Terrain roughness	**16** / *22*	**170** / *26*	**20** / *43*	**30** / *22*												
Lithology (rock type)	**192** / *117*	**153** / *150*	**139** / *276*	**89** / *117*	**119** / *117*											
Prox. to geol. contact	**55** / *26*	**22** / *32*	**22** / *53*	**30** / *26*	**27** / *26*	**87** / *150*										
Prox. to faults	**32** / *31*	**29** / *38*	**51** / *64*	**21** / *31*	**21** / *31*	**108** / *182*	**38** / *38*									
Prox. to drain. network	**71** / *26*	**85** / *32*	**22** / *53*	**67** / *26*	**26** / *26*	**104** / *150*	**37** / *32*	**18** / *38*								
Prox. to springs	**43** / *26*	**65** / *32*	**34** / *53*	**48** / *26*	**26** / *26*	**62** / *150*	**12** / *32*	**27** / *38*	**19** / *32*							
Prox. to temp. streams	**54** / *31*	**23** / *38*	**64** / *64*	**37** / *31*	**18** / *31*	**118** / *182*	**26** / *38*	**38** / *44*	**65** / *38*	**30** / *38*						
Prox. to perm. streams	**87** / *31*	**37** / *38*	**41** / *64*	**54** / *31*	**29** / *31*	**158** / *182*	**42** / *38*	**37** / *44*	**86** / *38*	**21** / *38*	**64** / *44*					
Prox. to all streams	**21** / *22*	**16** / *21*	**33** / *64*	**51** / *31*	**12** / *31*	**149** / *117*	**46** / *38*	**36** / *44*	**91** / *38*	**11** / *26*	**286** / *44*	**141** / *44*				
Topographic wetness	**62** / *22*	**21** / *26*	**16** / *43*	**28** / *22*	**16** / *22*	**51** / *117*	**13** / *26*	**13** / *31*	**39** / *26*	**28** / *26*	**19** / *31*	**18** / *31*	**24** / *31*			
Prox. to traffic infrastructure	**63** / *22*	**18** / *26*	**23** / *43*	**7** / *22*	**8** / *22*	**88** / *117*	**9** / *26*	**18** / *31*	**14** / *26*	**28** / *26*	**17** / *31*	**35** / *31*	**20** / *31*	**21** / *22*		
Land cover (A)	**30** / *22*	**35** / *26*	**30** / *43*	**34** / *22*	**18** / *22*	**116** / *117*	**22** / *26*	**27** / *31*	**46** / *26*	**22** / *26*	**24** / *31*	**88** / *31*	**33** / *31*	**19** / *22*	**12** / *22*	
Land cover (B)	**33** / *43*	**183** / *43*	**47** / *93*	**43** / *43*	**24** / *42*	**171** / *276*	**30** / *53*	**39** / *64*	**58** / *53*	**42** / *53*	**40** / *64*	**150** / *64*	**56** / *64*	**24** / *43*	**13** / *25*	**420** / *43*

Bold numbers are calculated and italic are tabulated Chi square values, respectively.
Values in green fields indicate accepted and in red fields rejected null hypothesis of conditional independence, respectively.

ever, four additional scenarios were defined, proving that only the anthropogenic group of landslide causal factors causes significant changes in the AUC values. Scenarios I, II and III resulted in almost equal AUC values compared to the optimal Scenario 0. In contrast, Scenario IV showed a success rate of only 79% and a prediction rate of 74%, which is significantly lower than the other scenarios.

The landslide susceptibility map created based on Scenario 0 using the Weight of Evidence method was classified into four classes (low, medium, high, and very high) using the cut-off values defined according to **Bernat Gazibara** (**2019**) (see **Figure 7**). The classification was done using the ROC curve derived from all landslides, both the modelling set and the validation set. **Fig-**
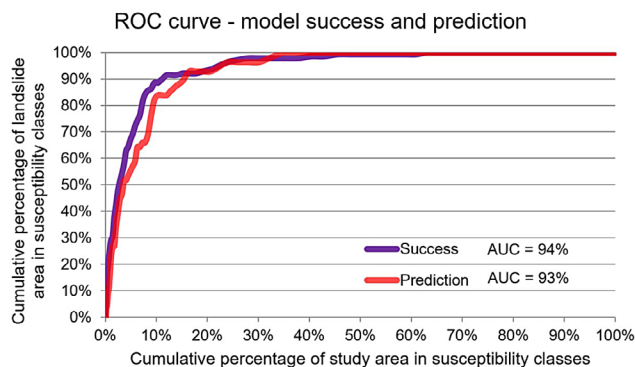

Figure 6: ROC curve analysis results for the rate of success and the rate of prediction for the final landslide susceptibility map

Table 5: Calculated and tabulated χ^2 values for filtered weight maps

	Slope orientation	Terrain roughness	Lithology (rock type)	Proximity to geological contact	Proximity to faults	Proximity to drainage network	Proximity to springs	Topographic wetness	Proximity to traffic infrastructure
Terrain roughness	**20.47**								
	42.98								
Lithology (rock type)	**138.77**	**138.05**							
	276.16	*117.06*							
Proximity to geological contact	**22.36**	**18.02**	**87.44**						
	53.49	*26.22*	*149.73*						
Proximity to faults	**50.72**	**21.41**	**108.48**	**25.10**					
	63.69	*30.58*	*181.84*	*37.57*					
Proximity to drainage network	**22.31**	**26.02**	**104.28**	**23.57**	**20.3**				
	53.49	*26.22*	*149.73*	*32.00*	*37.57*				
Proximity to springs	**34.02**	**25.51**	**61.96**	**12.15**	**30.72**	**19.12**			
	53.49	*26.22*	*149.73*	*32.00*	*37.57*	*32*			
Topographic wetness	**16.24**	**16.04**	**50.70**	**13.45**	**14.9**	**28.45**	**27.94**		
	42.98	*21.57*	*117.06*	*26.22*	*30.58*	*26.22*	*26.22*		
Proximity to traffic infrastructure	**23.42**	**8.41**	**88.07**	**8.54**	**20.92**	**13.79**	**29.26**	**21.28**	
	42.98	*21.67*	*117.06*	*26.22*	*30.58*	*26.22*	*26.22*	*21.67*	
Land cover (B)	**46.6**	**24.3**	**170.86**	**29.68**	**46.43**	**41.82**	**41.83**	**24.06**	**13.12**
	93.22	*41.98*	*276.16*	*53.49*	*63.69*	*53.49*	*53.49*	*42.98*	*24.98*

Bold and italic figures are calculated and tabulated Chi square values, respectively.
Values in green fields indicate accepted and in red fields rejected null hypothesis of conditional independence, respectively.

Table 6: Used weight maps and AUC rates for defined scenarios

Group of landslide causal factor	Weight maps	Scenarios				
		0	I	II	III	IV
Geomorphological	Slope orientation	+	-	+	+	+
	Terrain roughness	+	-	+	+	+
Geological	Lithology (rock type)	+	+	-	+	+
	Proximity to geological contact	+	+	-	+	+
	Proximity to faults	+	+	-	+	+
Hydrological	Proximity to drainage network	+	+	+	-	+
	Proximity to springs	+	+	+	-	+
	Topographic wetness	+	+	+	-	+
Anthropogenic	Land cover (B)	+	+	+	+	-
	Proximity to traffic infrastructure	+	+	+	+	-
AUC success rate (%)		94	93	94	94	79
AUC prediction rate (%)		93	92	93	94	74

ure 8 shows the final landslide susceptibility map of the City of Karlovac, and according to this map, 227.91 km² or 57.05% of the study area exhibits a low landslide susceptibility, 82.41 km² or 20.63% of the study area exhibits a medium landslide susceptibility, 53.07 km² or 13.28% of the study area exhibits a high landslide susceptibility and 36.09 km² or 9.03% of the study area exhibits a very high landslide susceptibility.
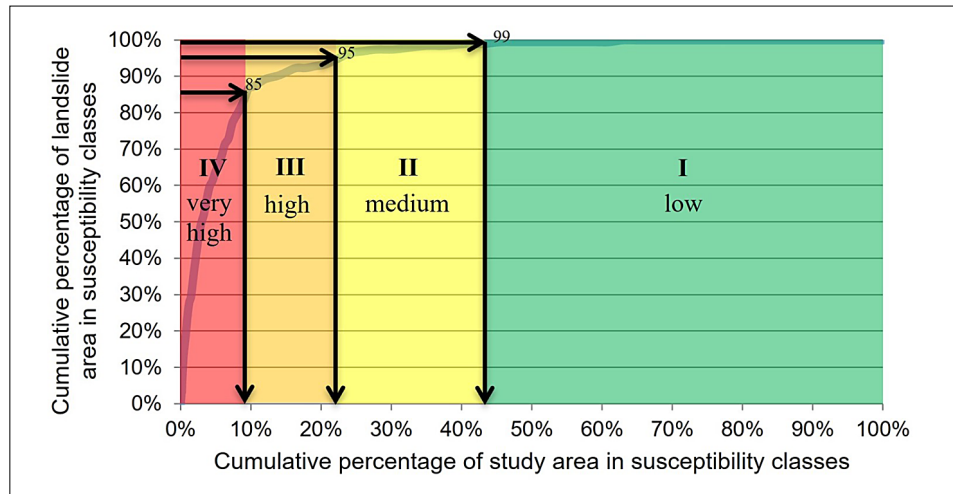
Figure 7: Classification of the ROC curve for the landslide susceptibility map according to the criteria from **Bernat Gazibara (2019)**
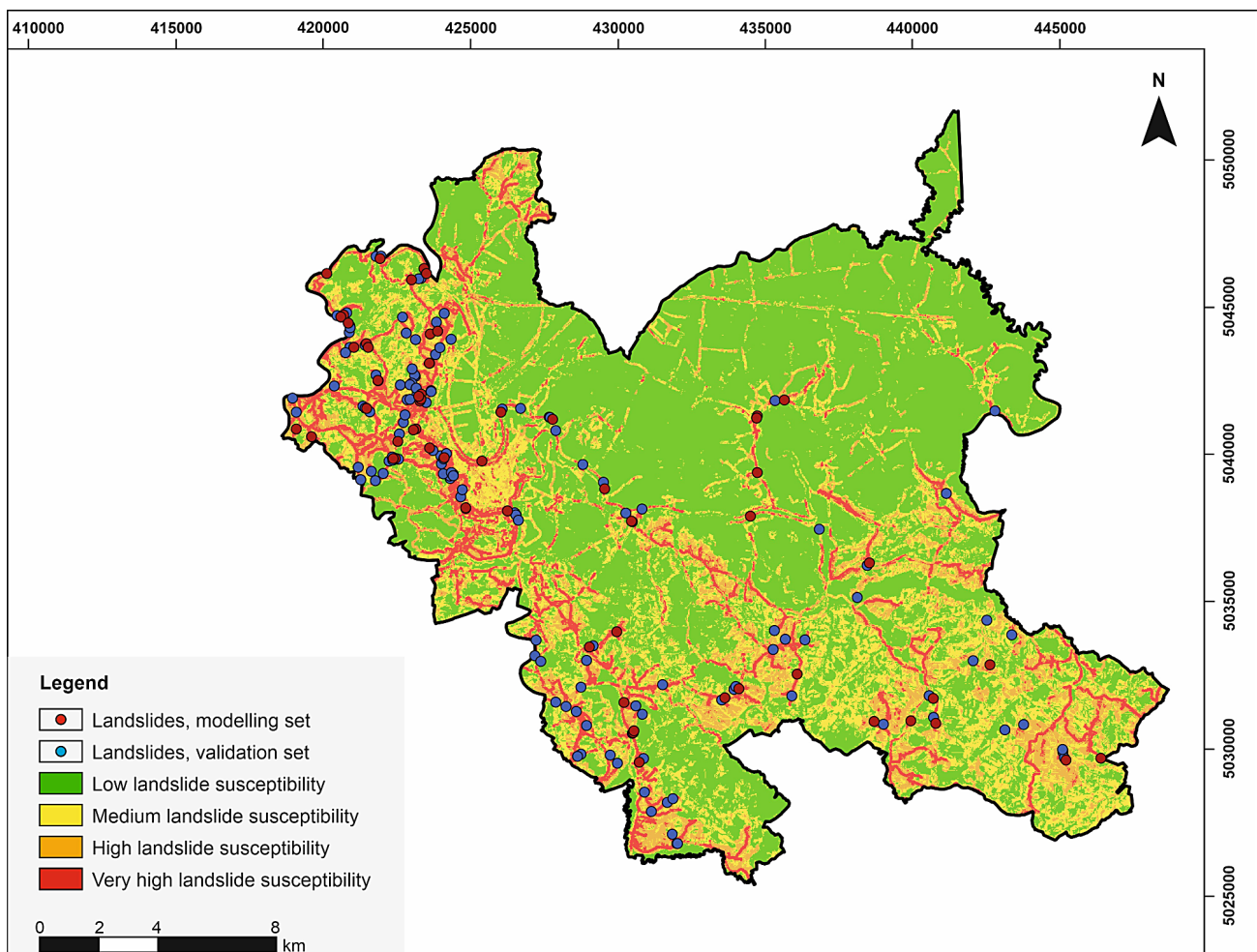

Figure 8: Landslide susceptibility of the City of Karlovac in a scale of 1:250 000 created by the Weight of Evidence method

5. Discussion

The proposed methodology to assess landslide susceptibility at a 1:100 000 scale is based on a bivariate method calibrated on a modelling set of landslides and tested by a validation set of landslides. The limitation of the used landslide inventory of the City of Karlovac is that it was compiled based on information collected by the municipal warden or citizens. It mainly contains reported landslides that caused damage to either buildings or infrastructures. This means that numerous landslides in green areas (forests, pastures, etc.) are missing from

the inventory. The mean landslide density of 0.48 landslides/km² at the area of the City is significantly lower than expected in terrains of similar geoenvironmental conditions (**Bernat Gazibara et al., 2019**). However, since landslides are distributed across the whole study area, for the purpose of this research, which is a preliminary landslide susceptibility map, the inventory is proven to be representative.

Modelling was started with 17 weight maps, followed by a pairwise CI test which resulted in a dependence of numerous combinations between weight map pairs. The main reason for this is that several weight maps included similar information and needed to be filtered out and excluded from the modelling. Further filtering and corrections lowered the CI violation to its minimum, ending up with only 3 out of 45 possible combinations showing dependence. The proposed method resulted in satisfactory AUC values for both success and prediction rates even though the modelling was done without a slope gradient map, commonly used in landslide susceptibility modelling. This proves that reducing the CI violating, i.e. decreasing the distortion of the results in a bivariate method, can be successfully performed by using a pairwise CI test without losing the performance of the model measured in AUC values.

Therefore, the final landslide susceptibility map was selected based on a maximum weight map, which contained minimum conditional dependence. Usage of 10 unique landslide causal factors with a significant number of classes in each provided that the final zonation has a detailed range of information. Final landslide susceptibility map zonation greatly influences its application, because the distribution of the zones could have an effect on spatial planning and land use management. The western and southern parts of the study area present a good transition from low to very high landslide susceptibility zones, as well as equal zone distribution. On the other hand, the north-eastern and central parts of the study area are generally classified as a low landslide susceptibility zone, which is expected considering the landslide causal factors at the area. The mentioned areas are predominately plain terrains where landslides are unlikely to occur. However, even in such areas, in a much lesser surface area, high and very high landslide susceptibility zones are distinguishable.

In this paper, map zonation was done using the ROC curve cut-off values defined by **Bernat Gazibara (2019)**, which resulted in a highly accurate and reliable classified landslide susceptibility map. Only 9% of the study area classified as very high landslide susceptibility contains 85% of mapped landslides, making it an efficient ratio pointing out the most susceptible areas. Therefore, additional zonation methods were not applied in this study since the mentioned method provided satisfactory information about specific areas in the City of Karlovac regarding landslide susceptibility. However, it is important to point out the importance of the zonation

method since different methods can result in very different zone distributions, leading to different map interpretation and its application. Such is the case with the proximity to traffic infrastructure, where the high influence of a single class shown in the Weight of Evidence analysis is well preserved even after the final overlapping of all weight maps proving that even a single factor can greatly impact the final zonation map.

Four additional scenarios were defined to test the influence of each group of landslide causal factors on the model performance. The results showed a direct link between the anthropogenic group of landslide causal factors and the AUC values. It is the only scenario that resulted in significantly different results compared to the final Scenario 0. Removing proximity to traffic and land use (B) resulted in far worse results in the AUC values, which is expected since 50 to 100 m proximity to traffic class in the proximity to traffic weight map has a significant W_{map} value. Since the landslide inventory mainly consists of landslides near the traffic infrastructure, the AUC values are directly linked to the landslide inventory. This observation proves how certain classes of weight maps can directly influence the quality of landslide susceptibility modelling because of their direct correlation to the landslide inventory, i.e. proving the significance of using a representative landslide inventory. Also, using a representative proximity to traffic weight map, which proved to be an important precondition for the occurrence of landslides, should be completed by roads from satellite images on a larger scale in order to deliver representative W_{map} values. The importance of a representative landslide inventory and representative weight maps is crucial to receive detailed results and high precision conclusions regarding certain geofactors and their relevance to landslide susceptibility. Also, using contrast and studentized contrast in the classification process would allow for the definition of different breakpoints when creating factor maps, however, in this paper, classes were defined expertly. Different breakpoints, i.e. the domain of each class in the weight maps leads to different landslide susceptibility modelling, which was not studied in this paper. According to **Neuhäuser et al. (2011)**, contrast and studentized contrast allow the classification to reflect the original spatial association of landslide causal factors and the landslides.

6. Conclusions

This paper has demonstrated the necessity of using specific and adapted procedures for indirect landslide susceptibility assessment by bivariate methods, especially at a 1:100 000 scale, for complex environments with some uncertainty in landslide inventory data. The proposed procedure, based on a limited amount of thematic data and a landslide inventory map, consists of: data collection, spatial data processing in GIS, development of weight maps and defining of geofactor classes,

analysis of the impact of individual classes of geofactors on landslides, CI analysis and weight map filtering, development of landslide susceptibility maps, verification of the susceptibility maps, and reclassification of the final susceptibility map into four classes of landslide susceptibility. The novelty in the presented research is that a limited amount of thematic data and an incomplete landslide inventory map allows for the production of a preliminary landslide susceptibility map for usage in spatial planning.

A reliable landslide susceptibility map was derived based on the analysis of ten geofactors: slope aspect, terrain roughness, lithology (rock type), proximity to geological contacts, proximity to faults, topographic wetness, proximity to springs, proximity to drainage network, proximity to traffic infrastructure and land cover (B classification). Pairwise CI test proved to be a successful method as it excluded seven out of ten geofactors, greatly influencing the overall performance of the model. The final preliminary landslide susceptibility map has a success rate of 94% and a prediction rate of 93%. The results proved a good correlation between the used geofactors and the occurrence of landslides. Three out of four additional scenarios resulted in similar success and prediction rates demonstrating that even with fewer geofactor maps, i.e. having even more limited data the reliability of susceptibility modelling would remain satisfactory. An exception being the anthropogenic geofactor group closely related to the landslide inventory map, as explained in the previous section.

Susceptibility modelling was done with easily accessible and high cost-benefit ratio input data, defining a robust and reproducible procedure for preliminary landslide susceptibility assessments. Our work shows that applying the simple Weight of Evidence method in the statistical model can satisfactorily recognise landslide-prone areas in a complex environment on a small scale of 1:100 000. In case of more complete and more representative landslide data, as well as DEM of higher resolution, it would be possible to create a susceptibility map on a medium or large scale. Moreover, further analyses would be necessary to collect more detailed input data for all factor maps to create a more reliable landslide susceptibility map.

Considering the availability and resolution of spatial data used to analyse landslide susceptibility in the City of Karlovac, there are also limitations for applying this map. Namely, the derived preliminary landslide susceptibility map can be used as a basis for future research to narrow down the study area to a larger scale because it provides preliminary information about the study area on a small scale. Taking into consideration that 85% of the landslides are zoned in only 9.03% of the study area provides relevant information regarding the priorities for the City's administration management. Overlapping the zonation done in this paper with settlement boundaries can also provide information on a larger scale, pointing our settlements in high or very high risk zones of landslide hazard. Most of the City's urban area is in the high and very high landslide susceptibility zone, which implies the necessity of further landslide risk management. The derived landslide susceptibility map can be used as a guideline for selecting areas for landslide susceptibility, hazard and risk zonation on a larger scale. Further landslide research in the City of Karlovac will lead to a better understanding of landslide prone areas, which is crucial for improving land use policy and reducing damage to buildings and infrastructures.

Analyses performed in this study resulted in a final version of the preliminary landslide susceptibility map that can be used for informative purposes as a basis for select areas in conducting further spatial analyses of landslide hazards.

7. References

Agterberg, F.P., Bonham–Carter, G.F. and Wright, D.F. (1990): Statistical Pattern Integration for Mineral Exploration. In: Gaal, G., Merriam, D.F. (eds.): Computer Applications in Resource Estimation: Prediction and Assessment for Metals and Petroleum. – Pergamon Oxford, 1-21, 473 p. doi: 10.1016/B978-0-08-037245-7.50006-8

Benček, Đ., Jukovac, J., Magaš, N. and Šimunić, A. (1989): Osnovna geološka karta 1:100 000, List Karlovac *(Basic geological map scale 1:100 000, sheet Karlovac)*. Institut za geološka istraživanja, Zagreb.

Bernat Gazibara, S., Krkač, M., Vlahek, I., Pavlić K., Begić, H., Zekan, S., Sečanj M. and Mihalić Arbanas, S. (2018): Extreme precipitation events and landslides activation in Croatia and Bosnia and Herzegovina. In: Jemec Auflić, M., Mikoš, M., Verbovšek, T. (eds.): Proceedings of the 3rd Regional Symposium on Landslides in the Adriatic Balkan Region: Advances in Landslide Research. – Ljubljana: Geological Survey of Slovenia, 19-24, 160 p.

Bernat Gazibara, S. (2019): Metodologija izrade karata klizišta korištenjem digitalnoga modela terena visoke rezolucije u podsljemenskoj zoni Grada Zagreba (Methodology for landslide mapping using high resolution digital elevation model in the Podsljeme area (City of Zagreb)). Rudarsko-geološko-naftni fakultet, Sveučilište u Zagrebu, Zagreb, 257 p. *(in Croatian with English abstract)*

Bernat Gazibara, S., Krkač, M. and Mihalić Arbanas, S. (2019): Verification of historical landslide inventory maps for the Podsljeme area in the City of Zagreb using LiDAR-based landslide inventory. Rudarsko-geološko-naftni zbornik, 34, 1, 45-58. doi: 10.17794/rgn.2019.1.5

Bognar, A. (2001): Geomorfološka regionalizacija Hrvatske *(Geomorphological regionalisation of Croatia)*. Acta Geo-

graphica Croatica, 34, 7 – 29. *(in Croatian without English abstract)*

Bonham-Carter, G.F., Agterberg, F.P. and Wright, D.F. (1989): Weights of evidence modelling: a new approach to mapping mineral potential. In: Agterberg, F.P. and Bonham-Carter, G.F. (eds.): Statistical Applications in the Earth Sciences. – Geological Survey of Canada, 171–183, 604 p. doi:10.4095/128059

Bonham-Carter, G.F. (1994): Geographic Information Systems for Geoscientists: Modelling with GIS. Pergamon, Ottawa, 398 p.

Brab, E.E., Pampeyan, E.H. and Bonilla, M.G. (1972): Landslide susceptibility in San Mateo County, California. US Geological Survey Miscellaneous Field Studies Map, MF-360, Map at 1:62 500 scale. doi: 10.3133/mf360

Bukovac, J., Šušnjar, M., Poljak, M. and Čakalo, M. (1983): Osnovna geološka karta 1:100 000, List Črnomelj *(Basic geological map scale 1:100 000 sheet Črnomelj)*. Geološki Zavod Zagreb i Geološki Zavod Ljubljana.

Cantarino, I., Carrion, M.A., Gisbert, F.J.and Martínez Ibáñez, V. (2018): A ROC analysis-based classification method for landslide susceptibility maps. Landslides, 16, 265–282. doi: 10.1007/s10346-018-1063-4

Carrara, A., Pugliese-Carratelli, E. and Merenda, L. (1977): Computer based data bank and statistical analysis of slope instability phenomena, Zeitschrift für Geomorphologie, 21, 187-222.

Chung C.J.F. and Fabbri, A. (2003): Validation of spatial prediction models for landslide hazard mapping. Natural Hazards, 30, 451–472. doi: 10.1023/B:NHAZ.0000007172.62651.2b

Corominas, J., van Westen, C., Frattini, P., Cascini, L., Malet, J.P., Fotopolou, S., Catani, F., Van Den Eeckhaut, M., Mavrouli, O., Agliardi, F., Pitilakis, K., Winger, M.G., Pastor, M., Ferlisi, S., Tofani, V., Hervas, J. and Smith, J.T. (2013): Recommendations for the quantitative analysis of landslide risk. Bulletin of Engineering Geology and the Environment, 73, 209–263. doi: 10.1007/s10064-013-0538-8

Coe.A., Godt, J.W., Baum, R.L., Bucknam, R.C. and Michael, J.A. (2004b): Landslide susceptibility from topography in Guatemala. In: Lacerda, W.A., Ehrlich, M., Fontoura, S.A.B. and Sayao, A.S.F. (eds.): Landslides, evaluation & stabilization. Proceedings of the 9th international symposium on landslides, Rio de Janeiro. – Leiden, London, 69–79, 1794 p. doi: 10.1201/b16816-8

Dai, F.C., Lee, C.F., Li J. and Xu, Z.W. (2001): Assessment of landslide susceptibility on the natural terrain of Lantau Island, Hong Kong. Environmental Geology, 40, 381–391. doi: 10.1007/s002540000163

Dietrich, E.W., Reiss R., Hsu, M.L. and Montgomery, D.R. (1995): A process-based model for colluvial soil depth and shallow landsliding using digital elevation data. Hydrological Process, 9, 383–400. doi: 10.1002/hyp.3360090311

Državni zavod za statistiku, DZS (2011): Statistička izvješća – Popis stanovništva iz 2011 Godine *(Croatian Bureau of Statistics, Statistical reports –census of 2011). (in Croatian without English abstract)* URL: http://www.dzs.hr (accessed 13th December 2021)

European Environment Agency (EEA). Copernicus Land Monitoring Service. URL: https://land.copernicus.eu/imagery-in-situ/eu-dem/eu-dem-v1.1?tab=download (eudem_v11_E40N20.tif). (accessed 13th of December 2021)

Evans, J.S., Oakleaf, J., Cushman, S.A. and Theobald, D. (2014): An ArcGIS toolbox for surface gradient and geomorphometric modeling, version 2.0-0. URL: http://evansmurphy.wix.com/evansspatial (accessed 13th December 2021)

Fell R., Corominas J., Bonnard C., Cascini L., Leroi E. and Savage W.Z. (on behalf of the JTC-1 Joint Technical Committee on Landslides and Engineered Slopes) (2008a): Guidelines for landslide susceptibility, hazard and risk zoning for land use planning. Engineering Geology, 102, 85–98. doi: 10.1016/j.enggeo.2008.03.022

Fell R., Corominas J., Bonnard C., Cascini L., Leroi E. and Savage W.Z. (on behalf of the JTC-1 Joint Technical Committee on Landslides and Engineered Slopes) (2008b): Guidelines for landslide susceptibility, hazard and risk zoning for land-use planning. Engineering Geology, 102, 99–111. doi: 10.1016/j.enggeo.2008.03.014

Green, D.M. and Swets, J.A. (1966): Signal Detection Theory and Psychophysics. John Wiley, Oxford, 455 p.

Grubišić, A. (2004): Hi-kvadrat test i njegove primjene *(Chi-square test and its application)*. Fakultet elektrotehnike i računarstva, Sveučilište u Zagrebu, Zagreb, 27 p. *(in Croatian without English abstract)*

Guzzeti, F. (2006): Landslide Hazard and Risk Assessment. Mathematics-Scientific Faculty, University of Bonn, Bonn, 339 p.

Guzzeti, F., Galli, M., Reichenbach P., Ardizzone, F. and Cardinali, M. (1999): Landslide Hazard assessment in the Collazzone area, Umbria, Central Italy. Natural hazards and earth system sciences, 6, 1, 115-131. doi: 10.5194/nhess-6-115-2006

Guzzetti, F., Cesare Mondini, A., Cardinali, M., Fiorucci, F., Santangelo, M. and Chang, K.T. (2012): Landslide inventory maps: New tools for an old problem. Earth-Science Reviews, 112, 1-2, 42-66. doi : 10.1016/j.earscirev.2012.02.001

Guzzeti, F. (2021): On the Prediction of Landslides and Their Consequences. In: K. Sassa, Mikoš, M., Sassa, S., Bobrowsky, P.T., Takara, K. and Dang, K. (eds.): Understanding and Reducing Landslide Disaster Risk. WLF 2020. ICL Contribution to Landslide Disaster Risk Reduction. – Springer, Cham., 3-32, 641 p. doi: 10.1007/978-3-030-60196-6_1

Marković, M. (1983): Osnovi primenjene geomorfologije *(Basics of applied geomorphology)*. Geoinstitut Beograd, 173 p. *(in Serbian without English abstract)*

Mihalić Arbanas, S. and Arbanas, Ž. (2015): Landslides: A Guide to Researching Landslide Phenomena and Processes. In: Gaurina Međimurec, N. (eds.): Handbook of Research on Advancements in Environmental Engineering. – IGI Global, 474-510, 660 p. doi: 10.4018/978-1-4666-7336-6.ch017

Mihalić Arbanas, S., Sečanj, M., Bernat Gazibara, S., Krkač, M., Begić, H., Džindo, A., Zekan, S. and Arbanas, Ž. (2017): Landslides in the Dinarides and Pannonian Ba-

sin—from the largest historical and recent landslides in Croatia to catastrophic landslides caused by Cyclone Tamara (2014) in Bosnia and Herzegovina. Landslides, 14, 1861–1876. doi: 10.1007/s10346-017-0880-1

Madaš, N., Bukovac, J. and Benček, Đ. (1989): Osnovna geološka karta, tumač za List Karlovac *(Basic geological map scale 1:100 000, legend forsheet Karlovac)*. Institut za geološka istraživanja, Zagreb, 1989.

National Reference Centres Land Cover (NRC/LC). CORINE Land Cover dataset. URL: https://land.copernicus.eu/pan-european/corine-land-cover (CLC2018_CLC2012_V2018_20b2.gdb) (accessed 13th December 2021)

Neuhäuser, B., Damn, B. and Terhorst, B. (2012): GIS-based assessment of landslide susceptibility on the base of the Weight-of-Evidence model. Landslides, 9, 511–528. doi: 10.1007/s10346-011-0305-5

Open Street Map (OSM). URL: http://download.geofabrik.de/europe.html (croatia-latest-free.shp). (accessed 13th December 2021)

Porwal, M.K., Agarwal, S.K. and Khokhar, A.K. (2006): Effect of planting methods and intercrops on productivity and economics of castor (Ricinus communis)-based intercropping systems. Indian Journal of Agronomy, 51, 274-277.

Reichenbach, P., Rossi, M., Malamud, B., Mihir, M. and Guzzetti, F. (2018): A review of statistically based landslide susceptibility models. Earth-Science Reviews, 180, 60-91. doi: 10.1016/j.earscirev.2018.03.001

Riley, S.J., Degloria, S.D. and Elliot, R. (1999): A terrain ruggedness index that quantifies topographic heterogeneity. Intermountain Journal of Sciences, 5, 1-4.

Sabto, M. (1991): Probabilistic modelling applied to landslides in central Columbia using GIS procedures. ITC, Enschede, 26 p.

Soeters, R. and Westen, C.J. (1996): Slope instability Recognition, analysis and zonation. In: Turner, A.K. and Schuster, R.L. (eds.): Landslide: Investigations and Mitigation. Special Report, vol. 247. Transportation Research Board, National Research Council, National Academy Press, Washington, D.C. 129–177, 247 p.

Schmid, S., Bernoulli, D., Fügenschuh, B., Matenco, L., Schefer, S., Schuster, R., Tischler, M. and Ustaszewski, K. (2008): The Alpine-Carpathian-Dinaridic orogenic system: Correlation and evolution of tectonic units. Swiss Journal of Geosciences, 101, 139-183. doi: 10.1007/s00015-008-1247-3

Tokić, L. (2017): ROC krivulja - krivulja odnosa specifičnosti i osjetljivosti klasifikatora *(ROC curve - the specifity-sensibility relation curve of the classifier)*. Prirodoslovno-matematički fakultet, matematički odsjek, Sveučilište u Zagrebu, Zagreb, 56 p. *(in Croatian with English abstract)*

Tomljenović, B., Csontos, L., Marton, E. and Marton, P. (2008): Tectonic evolution of the northwestern Internal Dinarides as constrained by structures and rotation of Medvednica Mountains, North Croatia. Geological Society London Special Publications, 298, 145-167. doi: 10.1144/SP298.8

Van Westen, C.J. (1993): Application of Geographic Information Systems to Landslide Hazard Zonation. ITC Publication, Enschede, 286 p.

Van Westen, C.J. (2002): Use of weights of evidence modeling for landslide susceptibility mapping. ITC Publication, Enschede, 21 p.

Van Westen, C.J., Asch, T.W.J. and Soeters, R. (2006): Landslide hazard and risk zonation-why is it still so difficult? Bulletin of Engineering Geology and Environment, 65, 167-184. doi: 10.1007/s10064-005-0023-0

Van Westen, C.J., Castellanos, E. and Kuriakose, S. (2008): Spatial data for landslide susceptibility, hazard, and vulnerability assessment: An overview. Engineering Geology, 102, 112-131. doi: 10.1016/j.enggeo.2008.03.010

Walker, H.M. and Lev, J. (1953): Statistical Inference: Holt, Rinehart and Winston, New York, 510 p.

WMS server DGU, URL: https://geoportal.dgu.hr/. (accessed 13th December 2021)

Yin, K.L. and Yan, T.Z. (1988): Statistical prediction model for slope instability of methamorphosed rocks. In: Bonnard, C. (eds.): Proceedings of Fifth International Symposium on Landslides, Lausanne, vol. 2. – A.A. Balkema, 1269-1272

Zaninović, K., Gajić-Čapka, M., Perčec Tadić, M., Vučetić, M., Milković, J., Bajić, A., Cindrić, K., Cvitan, L., Katušin, Z., Kaučić, D., Likso, T., Lončar, E., Lončar, Ž., Mihajlović, D., Pandžić, K., Patarčić, M.., Srnec, L. and Vučetić, V. (2008): Klimatski atlas Hrvatske 1961 – 1990, 1971 – 2000. (*Climate atlas of Croatia 1961. – 1990., 1971. – 2000.*). Državni hidrometeorološki zavod, Zagreb, 200 p. (*in Croatian without English abstract*). URL: https://klima.hr/razno/publikacije/klimatski_atlas_hrvatske.pdf (accessed 13th December 2021)

SAŽETAK

Procjena podložnosti na klizanje na području grada Karlovca primjenom bivarijantne statističke metode

Za grad Karlovac provedena je preliminarna analiza podložnosti na klizanje u regionalnome mjerilu 1 : 100 000 primjenom bivarijantne statistike. Inventar klizišta koji je korišten u analizama izradila je gradska uprava na temelju zabilježenih klizišta koja su izazvala znatne štete na zgradama ili infrastrukturi u razdoblju od 2014. do 2019. godine. Analize su uključivale 17 geofaktora relevantnih za pojavu klizišta podijeljenih u četiri skupine: geomorfološki (nadmorska visina, nagib terena, orijentacija padine, zakrivljenost terena, hrapavost terena), geološki (litologija, udaljenost od geološke granice, udaljenost od rasjeda), hidrološki (udaljenost od drenažne mreže, udaljenost od izvora, udaljenost od privremenih, stalnih i svih potoka, vlažnost terena) i antropogeni (udaljenost od prometne infrastrukture, namjena zemljišta primjenom dviju klasifikacija). Primjenom metode Weights-of-Evidence (WoE) definirano je pet scenarija, pri čemu su korišteni različiti geofaktori. Rezultati analiza čine pet različitih karata podložnosti na klizanje. Najbolja karta podložnosti na klizanje odabrana je na temelju rezultata analize ROC krivulje, koja je korištena za dobivanje stupnja točnosti i predikcije svakoga scenarija. Doprinos je prikazanoga istraživanja u tome da korištenje ograničenih tematskih karata i nepotpune karte inventara klizišta omogućuje izradu preliminarne karte podložnosti na klizanje za korištenje u prostornome planiranju. Također, ova studija pruža raspravu o korištenoj metodi, geofaktorima, definiranim scenarijima i pouzdanosti rezultata. Konačna preliminarna karta podložnosti na klizanje izrađena je korištenjem deset geofaktora koji su zadovoljili test *pairwise* CI i klasificirana je u četiri klase: niska podložnost na klizanje (57.05 % površine), srednja podložnost na klizanje (20.63 % površine), visoka podložnost na klizanje (13.28 % površine), vrlo visoka podložnost na klizanje (9.03 % površine), te ima stupanj točnosti od 94 % i stupanj predikcije od 93 %, što je čini vrlo točnim izvorom preliminarnih informacija za područje istraživanja.

Ključne riječi:
klizište, procjena podložnosti, zonacija, bivarijantna statistička analiza, grad Karlovac

Author's contribution

This paper is an elaborated Master's thesis research of the author **Marko Sinčić** (Junior Researcher – Assistant, PhD fellow), who prepared the input data and performed analyses (bivariate statistics, contingency table, ROC curve). **Sanja Bernat Gazibara** (Postdoctoral Researcher) supervised the analyses, defined the research methodology and participated in the interpretation of the results. **Martin Krkač** (Associate Professor) and **Snježana Mihalić Arbanas** (Full Professor) participated in defining the paper's concept and gave suggestions for the discussion and the conclusion, and made a complete critical revision of the paper.